

The stability of fundamental constants

Azores Aug 2017
John Webb, UNSW/CMS
Cambridge



Illustration: Scientific American : *Inconstant Constants*, Barrow & Webb. Artist: J-F. Podevin, www.podevin.com

Main project collaborators:

- Matthew Bainbridge (Leicester)
- John Barrow (CMS, Cambridge)
- Bob Carswell (IoA, Cambridge)
- Chung-Chi Lee (DAMPT, Cambridge)
- Darren Dougan (PhD student UNSW)
- Vincent Dumont (Berkeley)
- Victor Flambaum (UNSW)
- Dinko Milakovic (PhD student, ESO)
- Gillian Nave (NIST, Colorado)
- Lydia Tchang-Brillet (Paris)
- Michael Wilczynska (PhD student UNSW)

Dimensionless ratios – things we can actually check

Quantity	Algebraic ratio	Numerical value	Related to
α_{EM}	$\frac{e^2}{4\pi\epsilon_0\hbar c}$	1/137.03599976	Strength of the electromagnetic force
α_{W}	$\frac{G_{\text{F}}m_p^2c}{\hbar^3}$	1.03×10^{-5}	Strength of the weak force
$\alpha_{\text{S}}(E)$	$\frac{g_s^2(E)}{\hbar c}$		Strength of the strong force
α_{G}	$\frac{Gm_p^2}{\hbar c}$	5×10^{-39}	Strength of the gravitational force
μ	$\frac{m_e}{m_p}$	5.44617×10^{-4}	
x	$g_p\alpha_{\text{EM}}^2\mu$	1.62×10^{-7}	
y	$g_p\alpha_{\text{EM}}^2$	2.977×10^{-4}	

Telescopes and instruments ~\$230M.

Keck Observatory
Mauna Kea, Hawaii

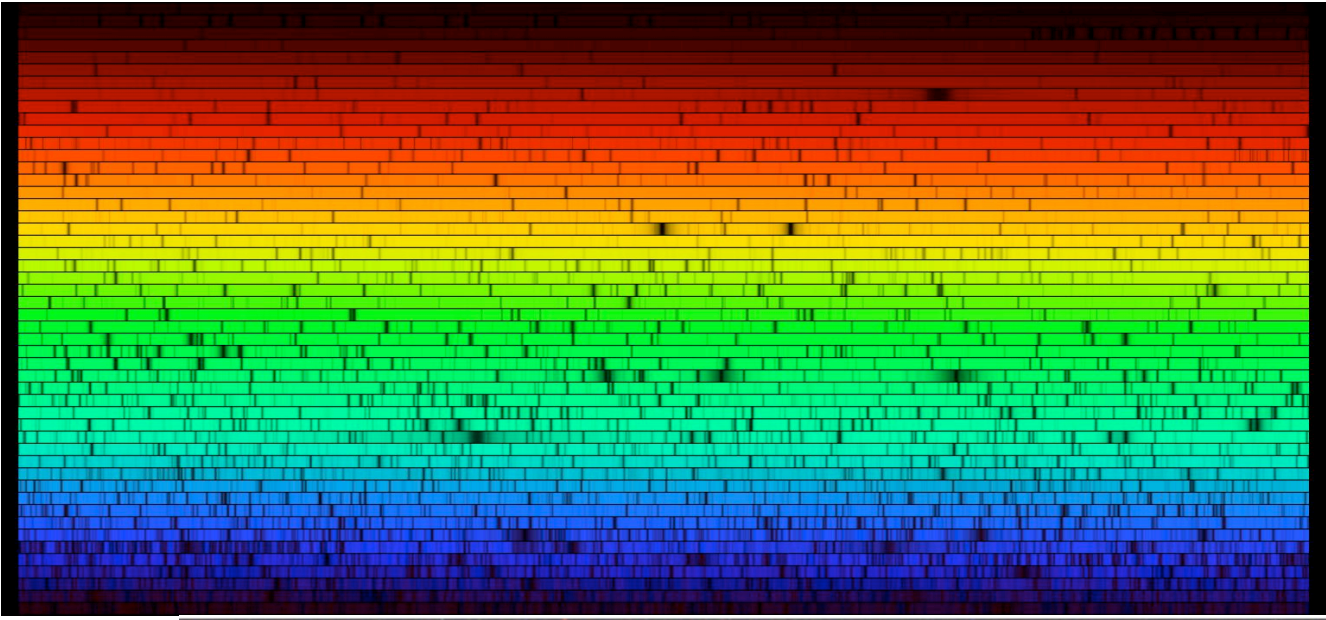


European Southern Observatory VLT
Paranal, Chile

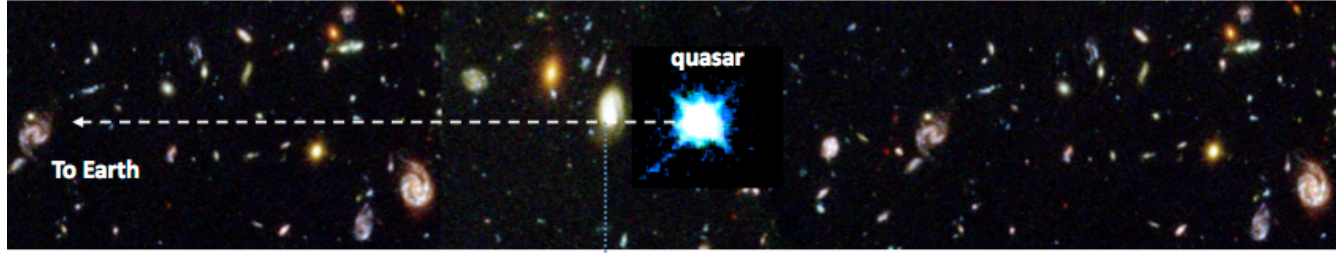
Telescopes and instruments ~\$470M.



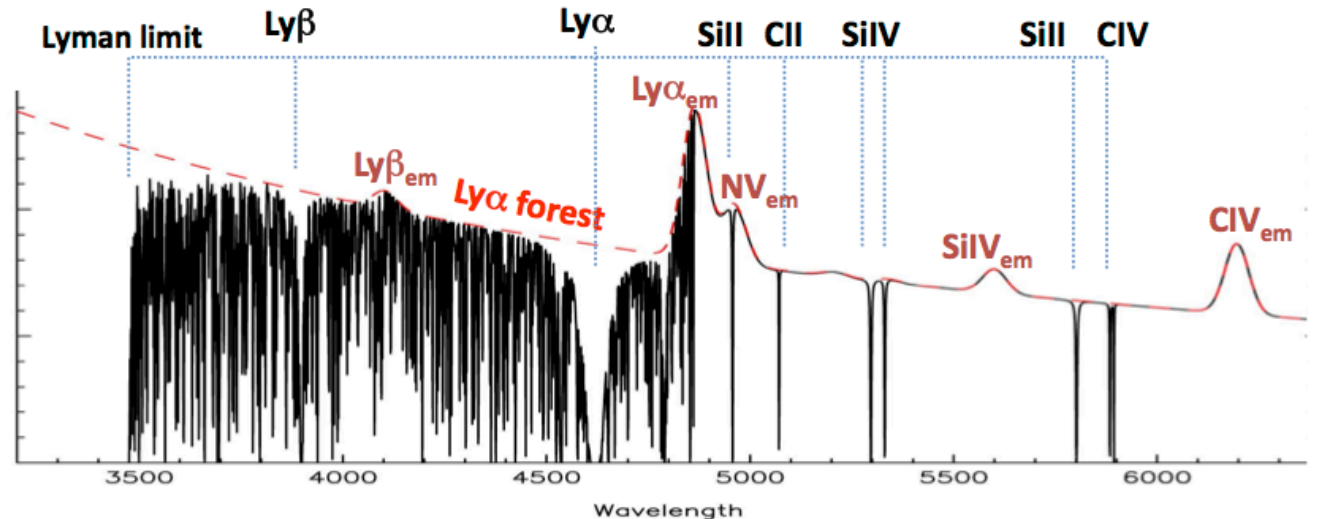
From raw data like this...
(the colours are artificial)



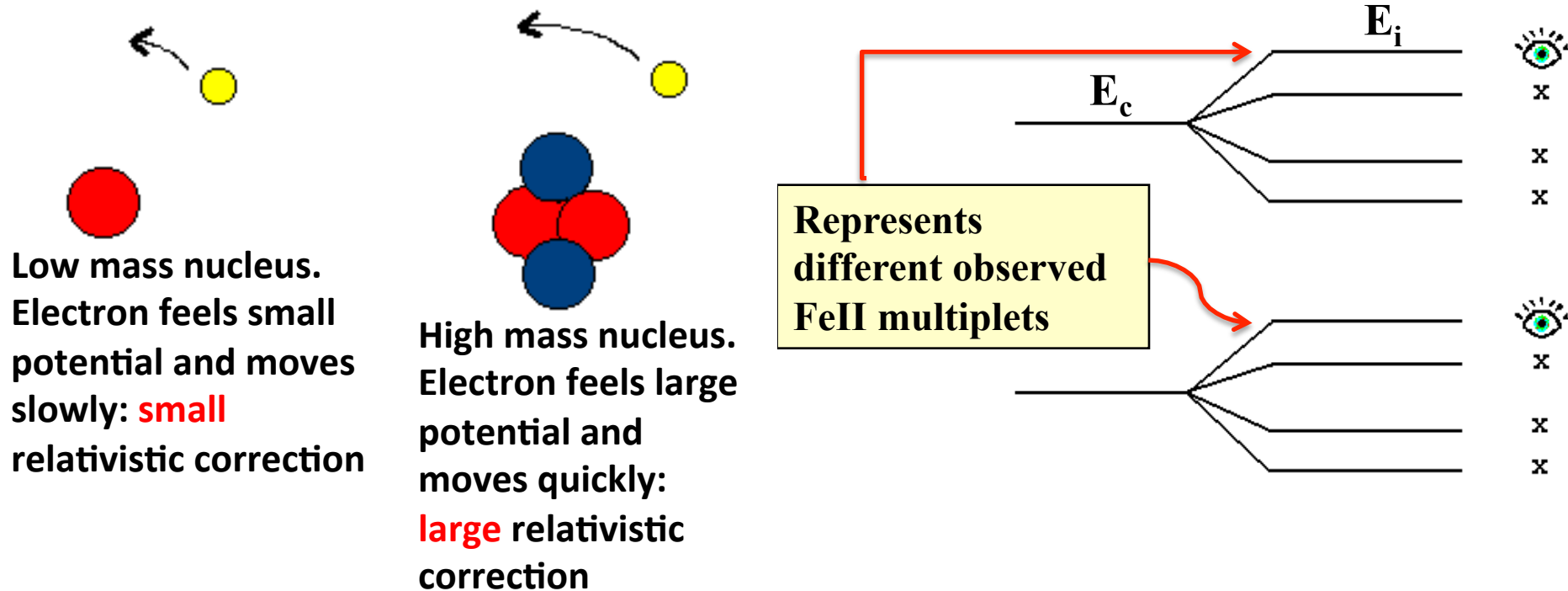
A 1-d spectrum is produced:



Transitions frequently seen include: HI, OI, SiII, CII, FeII, MgII, ZnII, CrII, NiII, CIII, CIV, SiIV, NV, OVI, H₂



The Many-Multiplet method – Relativistic Hartree-Fock calculations. Enables use of different multiplets simultaneously - *order of magnitude improvement over previous Alkali Doublet method*



- Ground state is most sensitive to variations in alpha so important to compare transitions from different multiplets, rather than alkali doublets
- Lots of multiplets are detected so statistics are good
- Different sensitivities to alpha (including opposite signs of shifts) create a unique pattern – difficult to emulate with a simple calibration distortion.

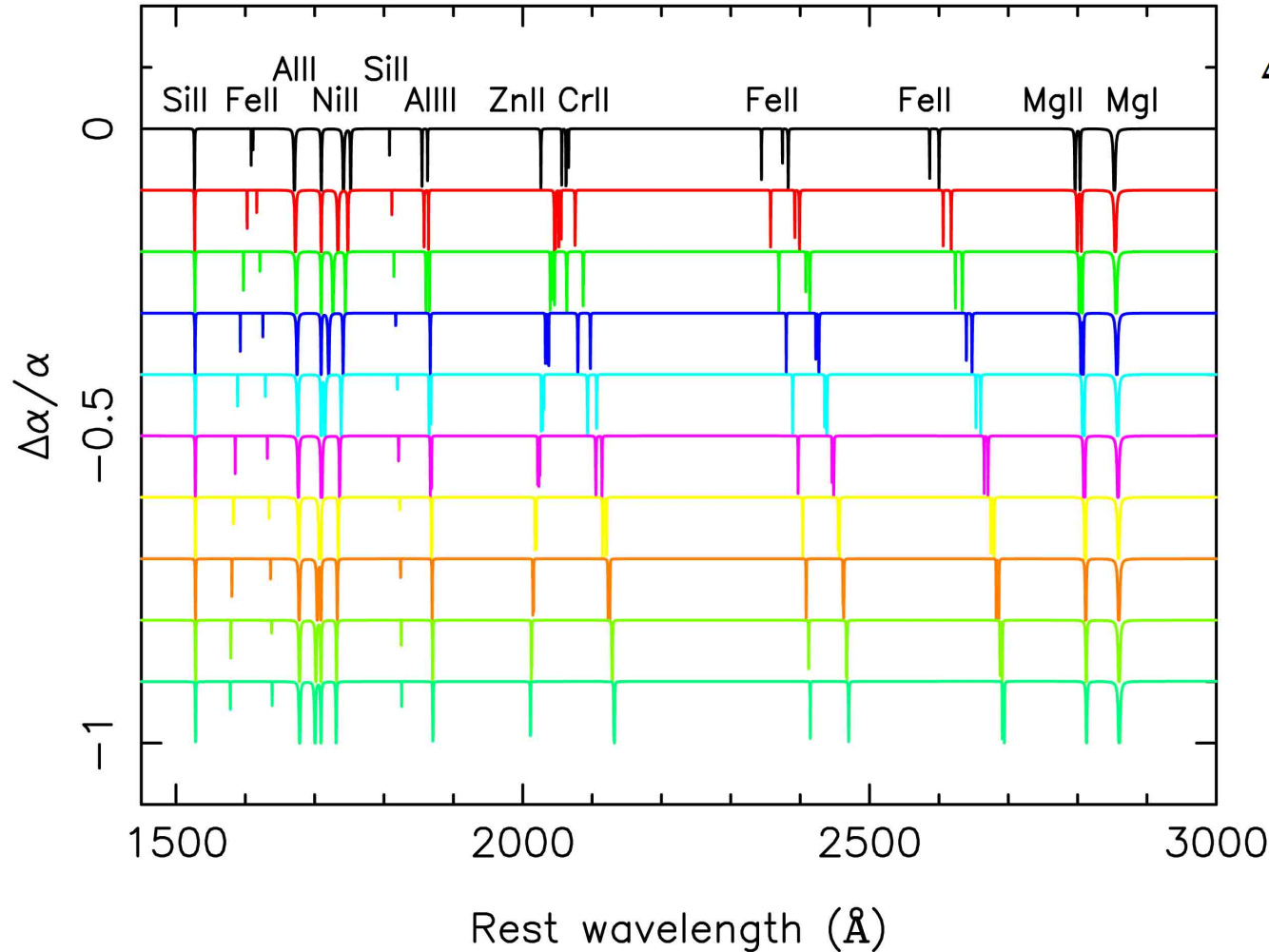
[Dzuba, Flambaum, Webb, *Phys.Rev.Lett.*, 82, 888, 1999](#)

[Webb, Flambaum, Churchill, Drinkwater, Barrow, *Phys.Rev.Lett.*, 82, 884, 1999](#)

Transitions shift in different directions and by different amounts – a unique pattern

$$\omega_z = \omega_0 + Q (\alpha_z^2 - \alpha_0^2) / \alpha_0^2$$

$$\Delta\alpha/\alpha = (\alpha_z - \alpha_0) / \alpha_0$$



Dzuba, Flambaum, Webb, *Phys.Rev.Lett.*, 82, 888, 1999

Webb, Flambaum, Churchill, Drinkwater, Barrow, *Phys.Rev.Lett.*, 82, 884, 1999

Spectral modelling

- VPFIT*. Fits multiple Voigt profiles using non-linear least-squares with tied parameters
- Can be up to several hundred free parameters
- Descent direction depends on derivatives of χ^2 with respect to each of the free parameters
- Finite difference derivatives or semi-analytic?
- No unique model - ever!
- Despite that, parameter solutions in fact *are* stable and reproducible (shown later)

* Carswell & Webb, <https://www.ast.cam.ac.uk/~rfc/vpfit.html>

1. basic equations

The intensity is evaluated by using the relation,

$$I_\nu = I_0 e^{-\tau_\nu}, \quad (1)$$

where $I_0 = 1$ is taken in the following calculations, and

$$\tau_\nu = \frac{\sqrt{\pi} e^2}{m_e c^2} \frac{\lambda^2 f_\lambda}{\Delta\lambda_D} H(a, u) = \tau_0 \frac{c}{b} H(a, u), \quad (2)$$

$$\Delta\lambda_D = \frac{b}{c} \lambda, \quad u = \frac{\lambda - \lambda_0}{\Delta\lambda_D}, \quad a \propto \frac{c}{b}. \quad (3)$$

2. parameters

$c = 3 \times 10^5$ km/s, $b = 30$ km/s, $a = 10^{-4}$ and $\lambda_0 = 1215.6701$ are used here.

3. equations in the figures/codes

The following notations are used in the following figures.

$$\Delta\lambda = \lambda - \lambda_0, \quad (4)$$

$$I_b = \frac{dI(a, u)}{db}, \quad I_b^{FDD} = \frac{I(a, u, b + \delta b) - I(a, u, b - \delta b)}{2\delta b}, \quad (5)$$

$$\delta I_b = \frac{I_b^{\text{lookup}} - I_b^{FDD}}{I_b^{\text{lookup}}} \quad (6)$$

where I_b^{lookup} is the derivative of $I(a, u)$ with respect to b from the lookup table, given by

$$I_b^{\text{lookup}} = \frac{dI_\nu}{db} = \frac{de^{-\tau_\nu}}{db} = -I_\nu \frac{d\tau_\nu}{db} = I_\nu \tau_0 \left(\frac{c}{b^2} H + \frac{ac}{b^2} \frac{\partial H}{\partial a} + \frac{cu}{b^2} \frac{\partial H}{\partial u} \right), \quad (7)$$

where $H(a, u)$, $\frac{\partial H}{\partial a}$ and $\frac{\partial H}{\partial u}$ are calculated from the lookup tables.

Fractional uncertainty in the derivative of the intensity as a function of finite derivative step-size

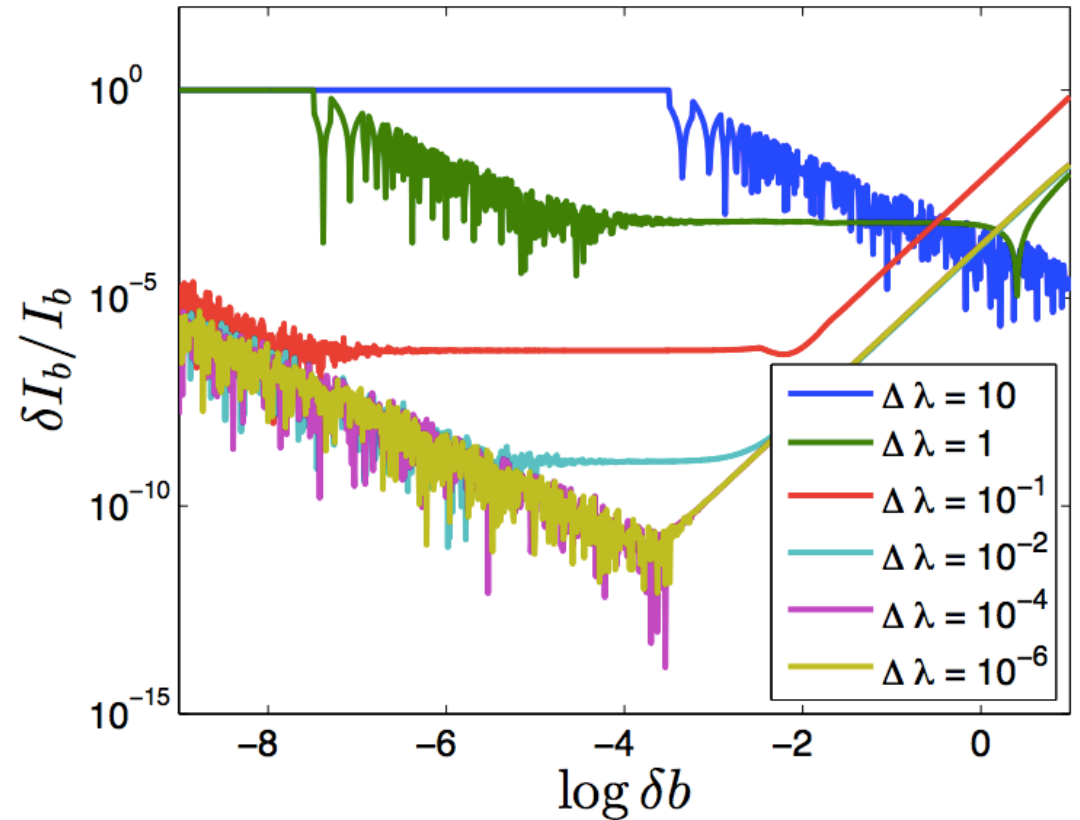
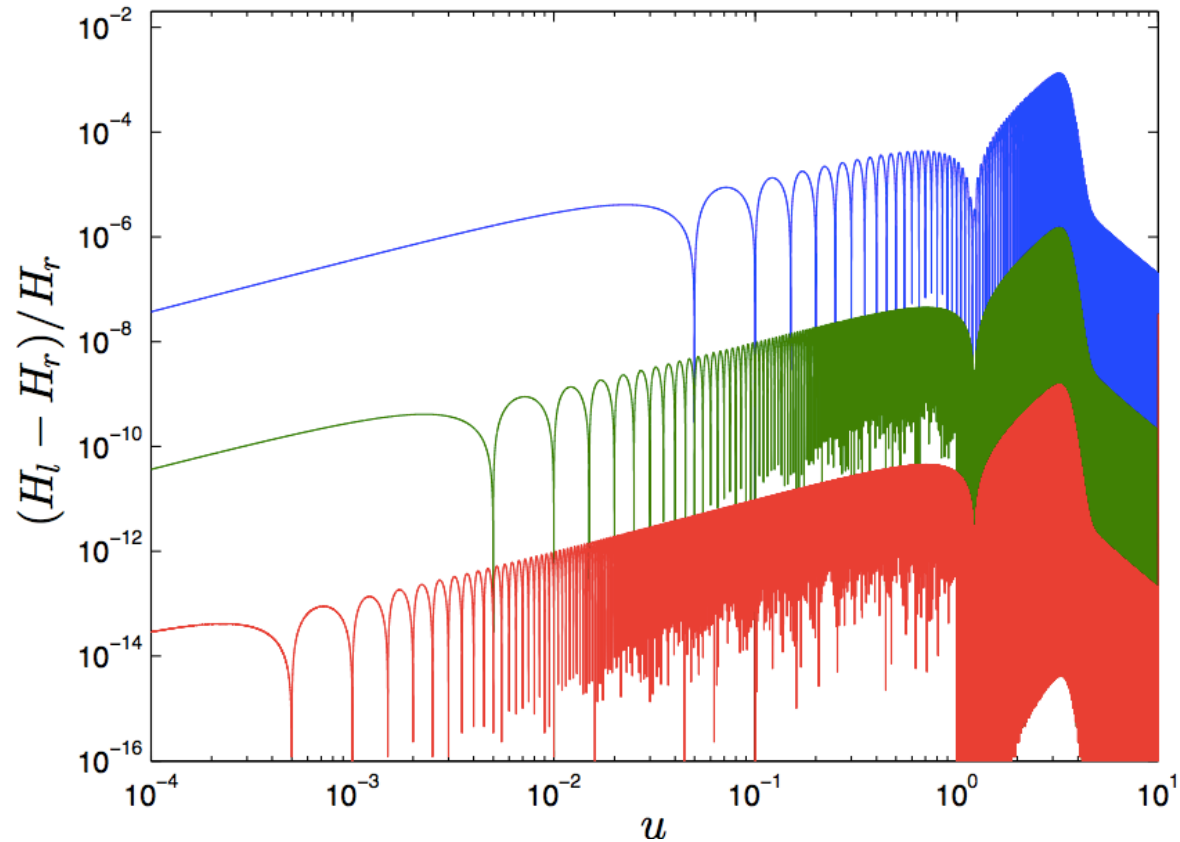


FIG. 1. We have used $\tau_0 = 10^{-4}$ in these plots. The first two plots show the absorption lines as functions of u and λ . The 3rd plot (second on the left) is dI/db . It is amazingly the derivative of I increases near the line center. In the 4th plot (second on the right), I show the numerical error from the finite step differential derivative method with the step size of $\delta b = 0.001$ (blue line), 0.01 (green line), 0.1 (red line), 1 (cyan line), 10 (magenta line) with the unit km/s . The last figure is the numerical error from FDD as functions of step size δb with different wavelength. The blue, green, red, cyan, magenta and yellow lines correspond to $\Delta \lambda = \lambda - \lambda_0 = 10, 1, 10^{-1}, 10^{-2}, 10^{-4}$ and 10^{-6} .

Fractional uncertainty on $H(u)$ (at fixed a) as a function of look-up table resolution



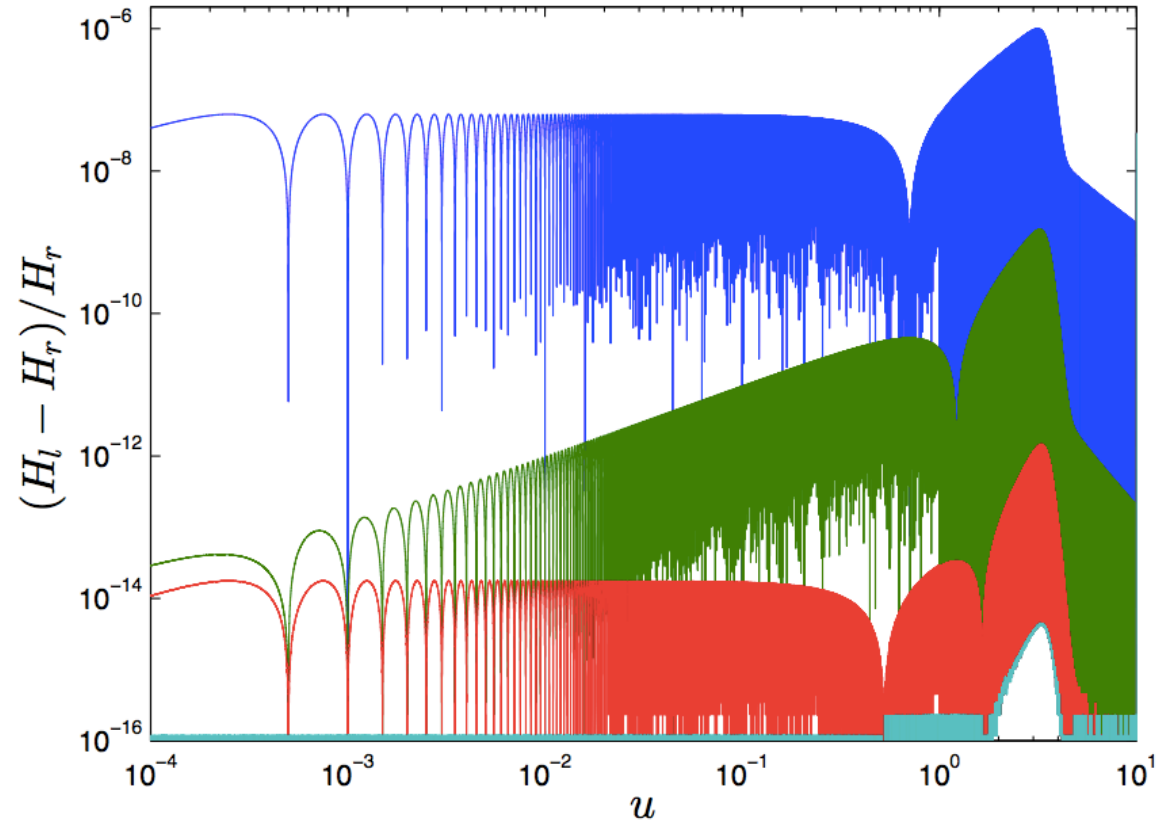
$\delta H(a, u)$ as functions of u with the 3 points interpolation method

Blue line: 200 data points in the lookup table.

Green line: 2,000 data points in the lookup table.

Red line: 20,000 data points in the lookup table.

Fractional uncertainty on $H(u)$ (at fixed a) as a function of look-up table interpolation



$\delta H(a, u)$ as functions of u with 20,000 data points in the lookup table

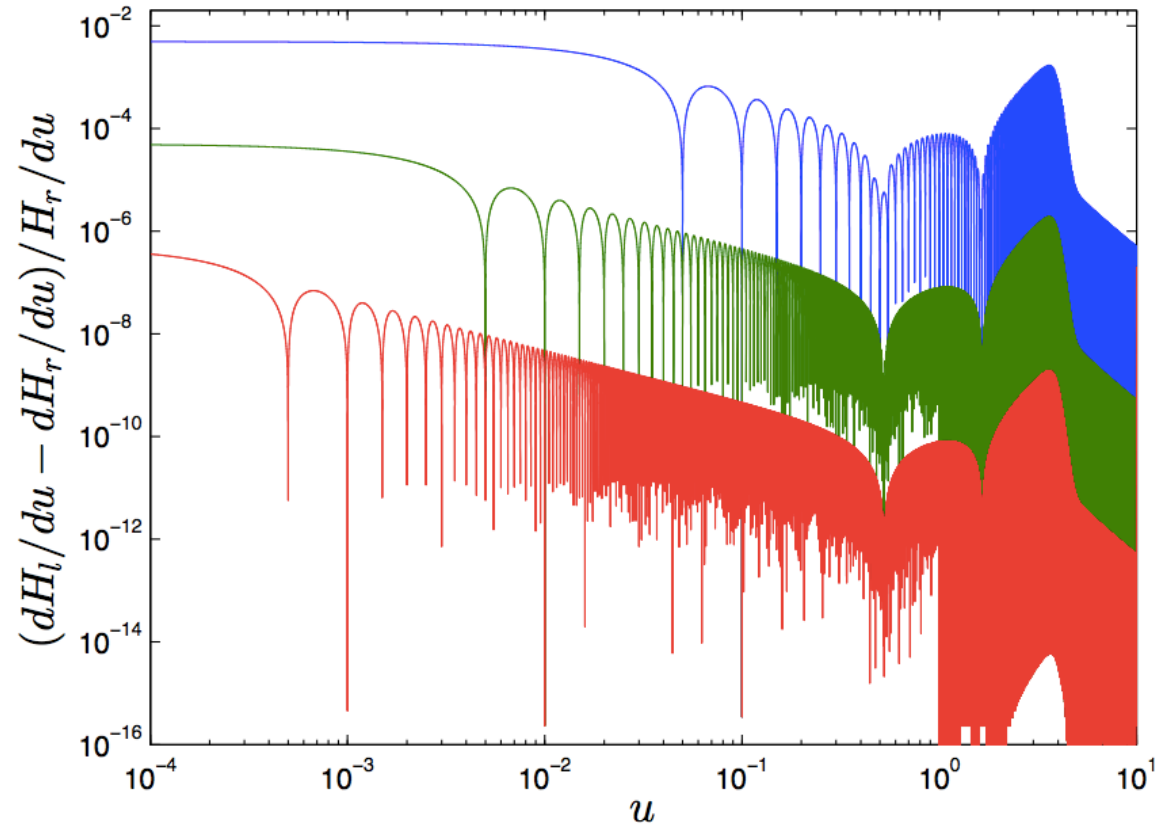
Blue line: 2 points interpolation.

Green line: 3 points interpolation.

Red line: 4 points interpolation.

Cyan line: 6 points interpolation.

Fractional uncertainty on derivative of $H(u)$ (at fixed a) as a function of look-up table resolution



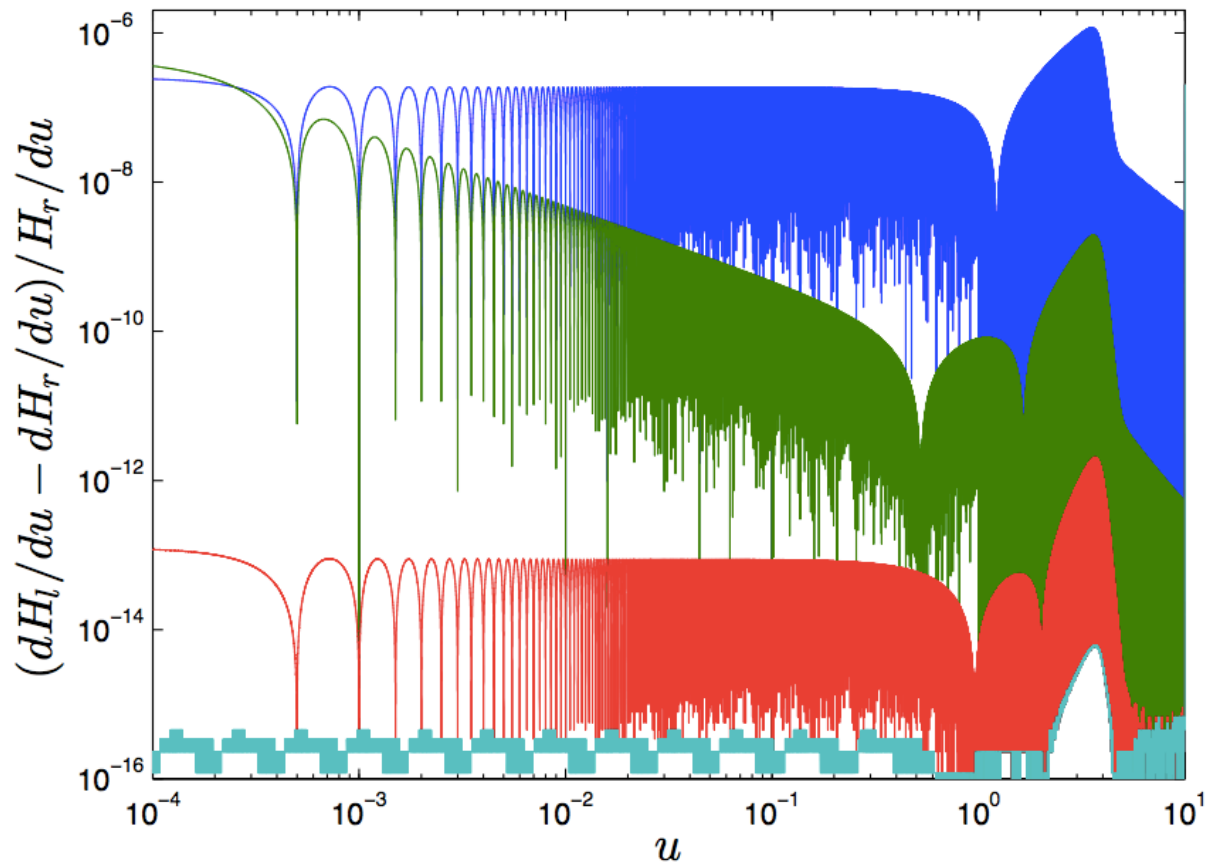
$\delta \left(\frac{dH}{du} \right)$ as functions of u with the 3 points interpolation method

Blue line: 200 data points in the lookup table.

Green line: 2,000 data points in the lookup table.

Red line: 20,000 data points in the lookup table.

Fractional uncertainty on derivative of $H(u)$ (at fixed a) as a function of look-up table interpolation



$\delta \left(\frac{dH}{du} \right)$ as functions of u with 20,000 data points in the lookup table

Blue line: 2 points interpolation.

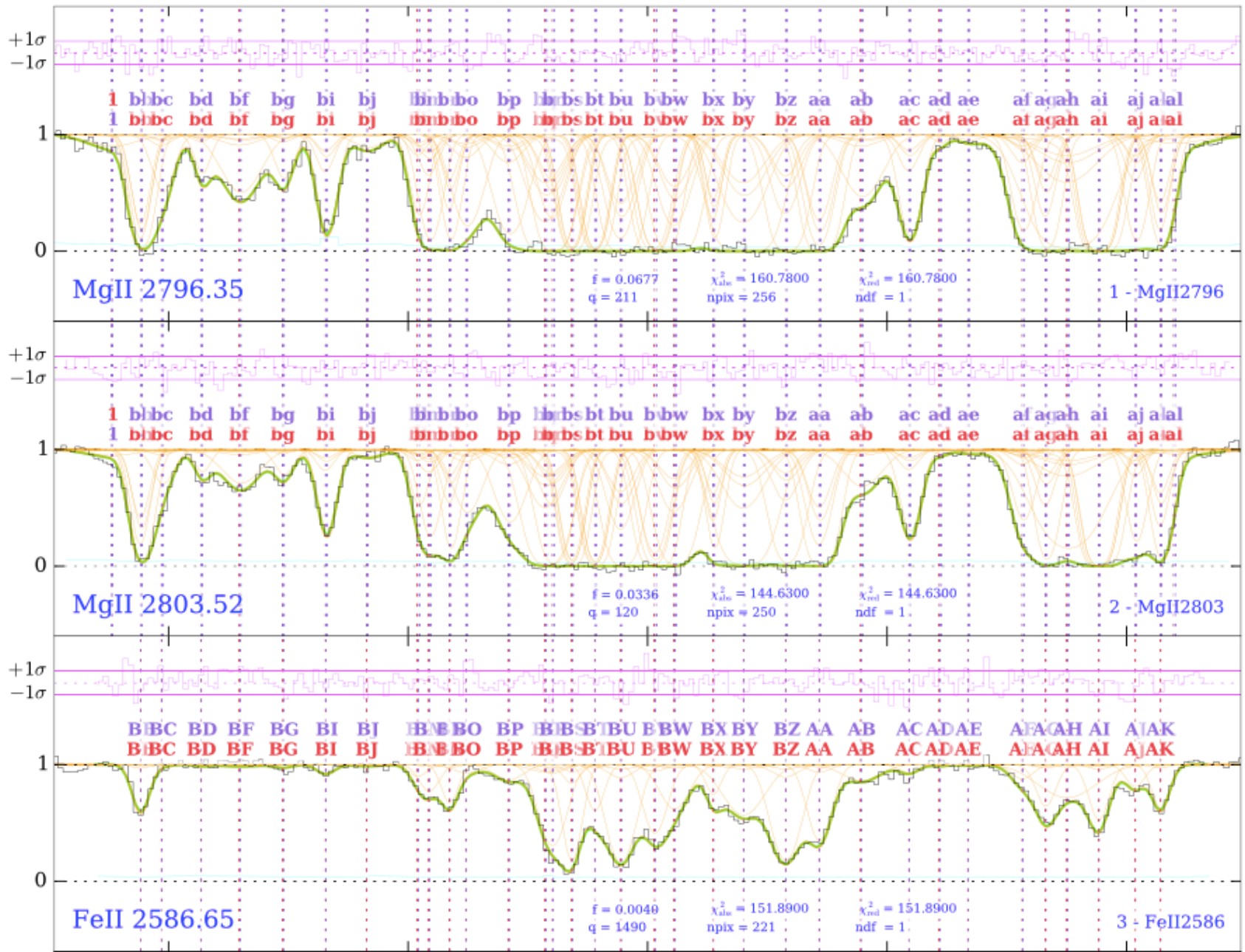
Green line: 3 points interpolation.

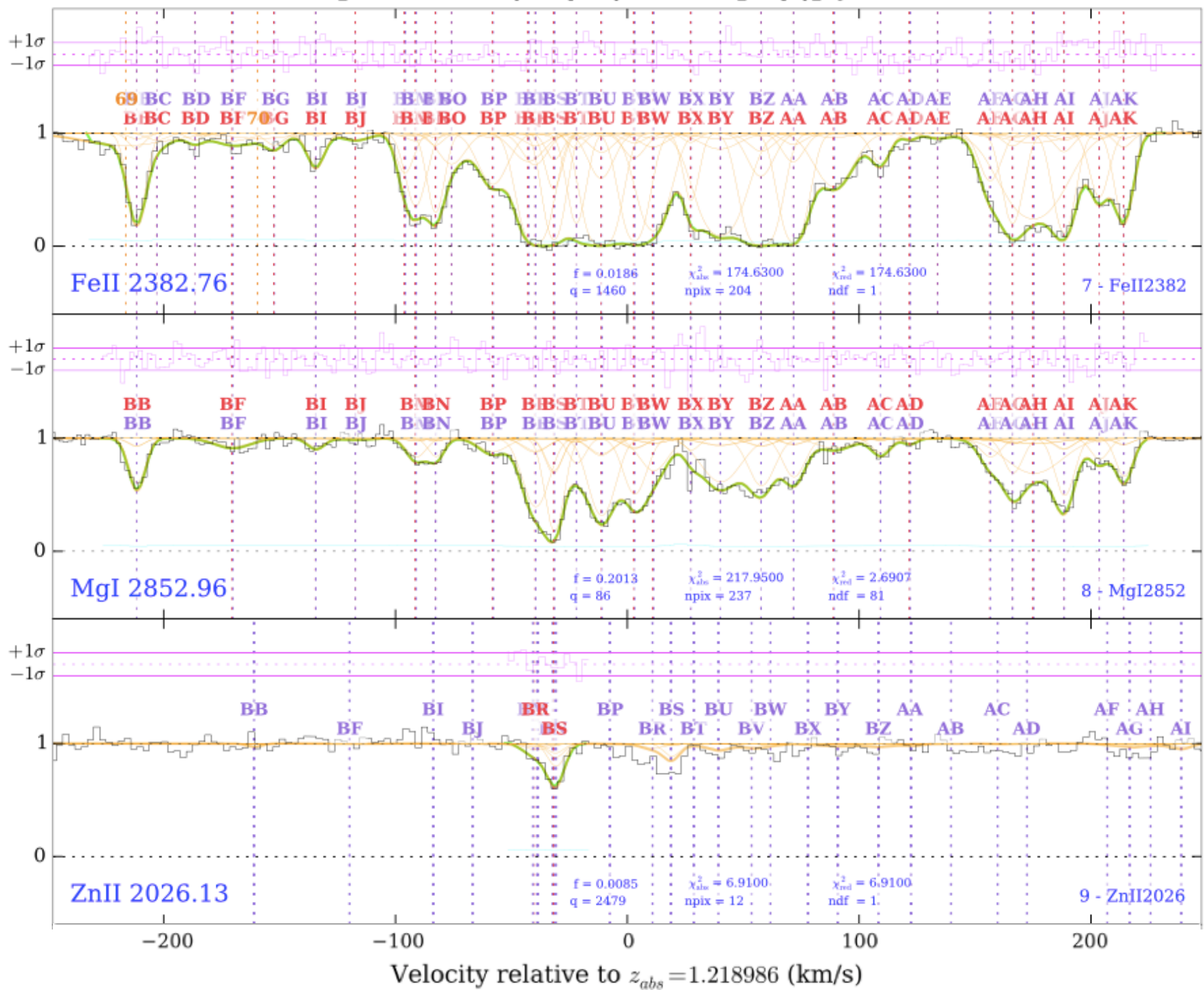
Red line: 4 points interpolation.

Cyan line: 6 points interpolation.

Lessons from the above:

1. Just because a method seems “well established”, it is sometimes important to go back and check the basics
2. Make sure you use enough data when using polynomials to interpolate (method used in this case was Lagrange interpolation)
3. Look-up tables are used commonly for calculating complex expressions that would otherwise require computationally time-demanding numerical integrations
4. VPFIT is being improved to significantly improve the precision of Voigt function $H(a,u)$ calculations and the derivatives of the Voigt function. Both are used internally. Both are important for optimal analysis of high signal-to-noise, high resolution quasar spectra.



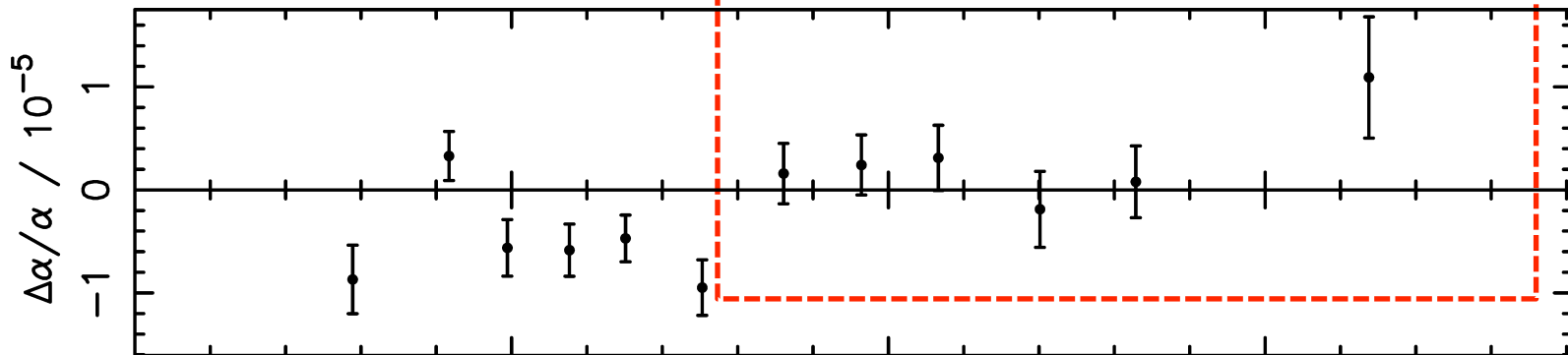


α in two hemispheres

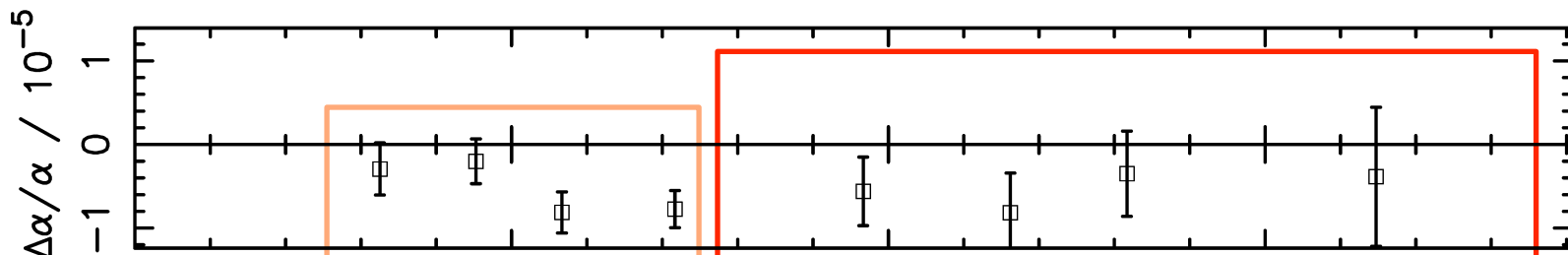
King, Webb, Murphy, Flambaum, Carswell, Bainbridge, Wilczynska, Koch, . MNRAS, 422, 3370, 2012

Webb; King, Murphy, Flambaum, Carswell, Bainbridge, PRL, 107, 191101, 2011

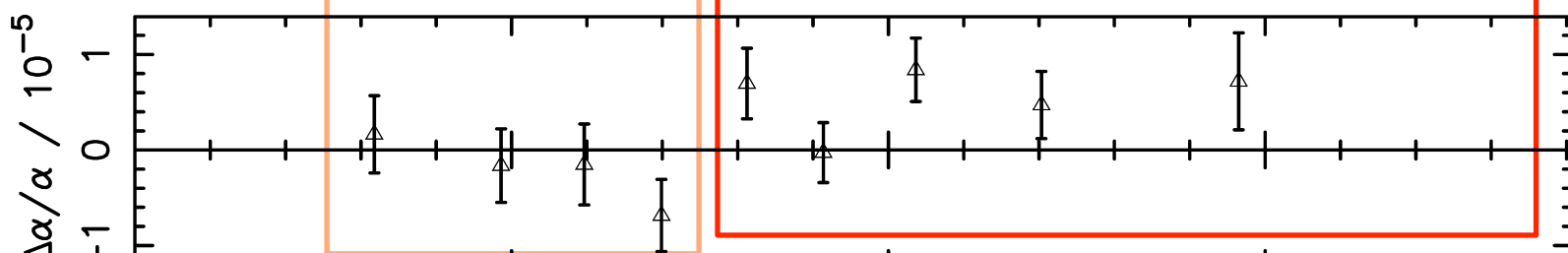
VLT +
Keck



Keck



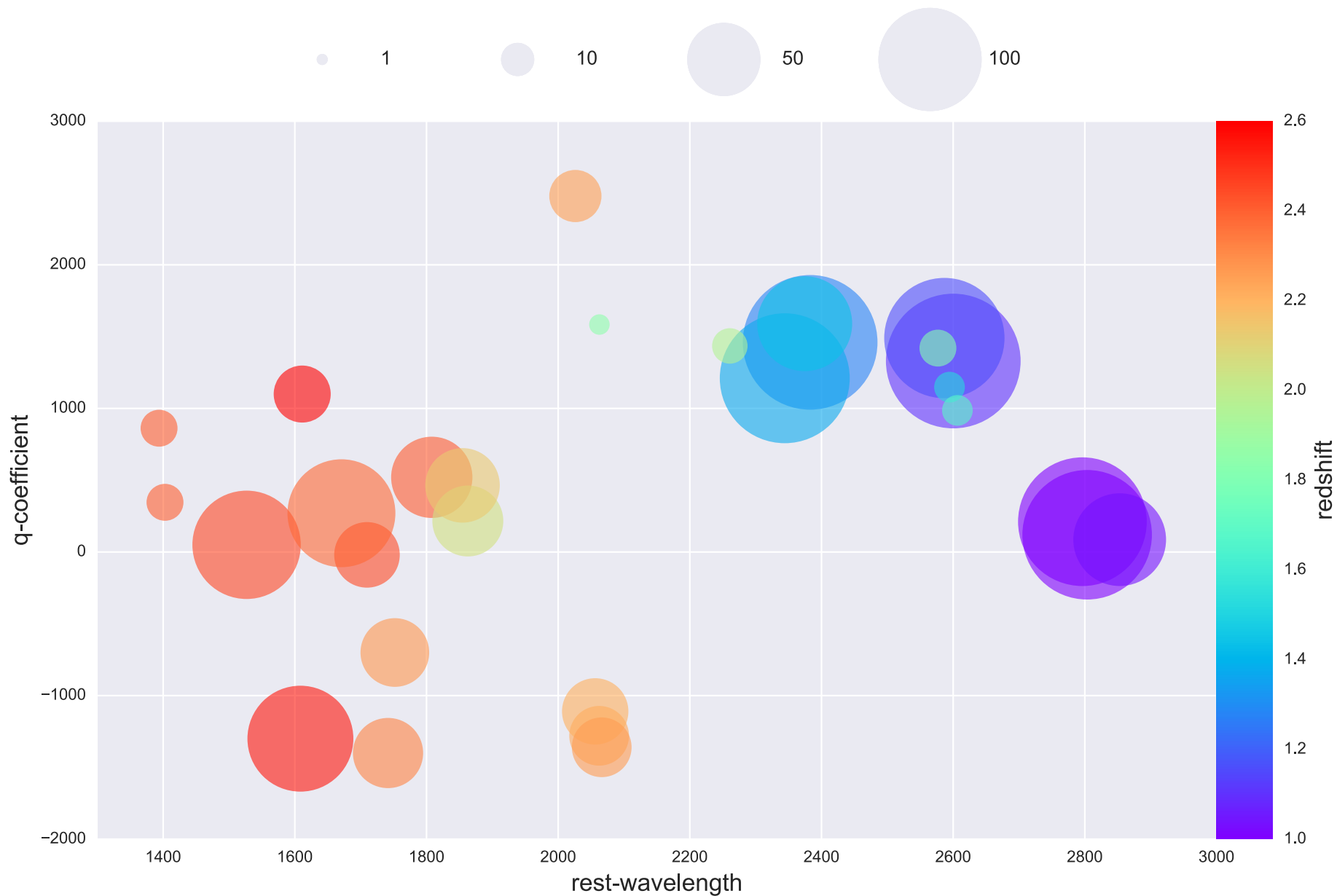
VLT



$$\langle \Delta\alpha/\alpha \rangle_{z>1.8} = -0.74 \pm 0.17 \times 10^{-5} \text{ Keck} \\ +0.61 \pm 0.20 \times 10^{-5} \text{ VLT}$$

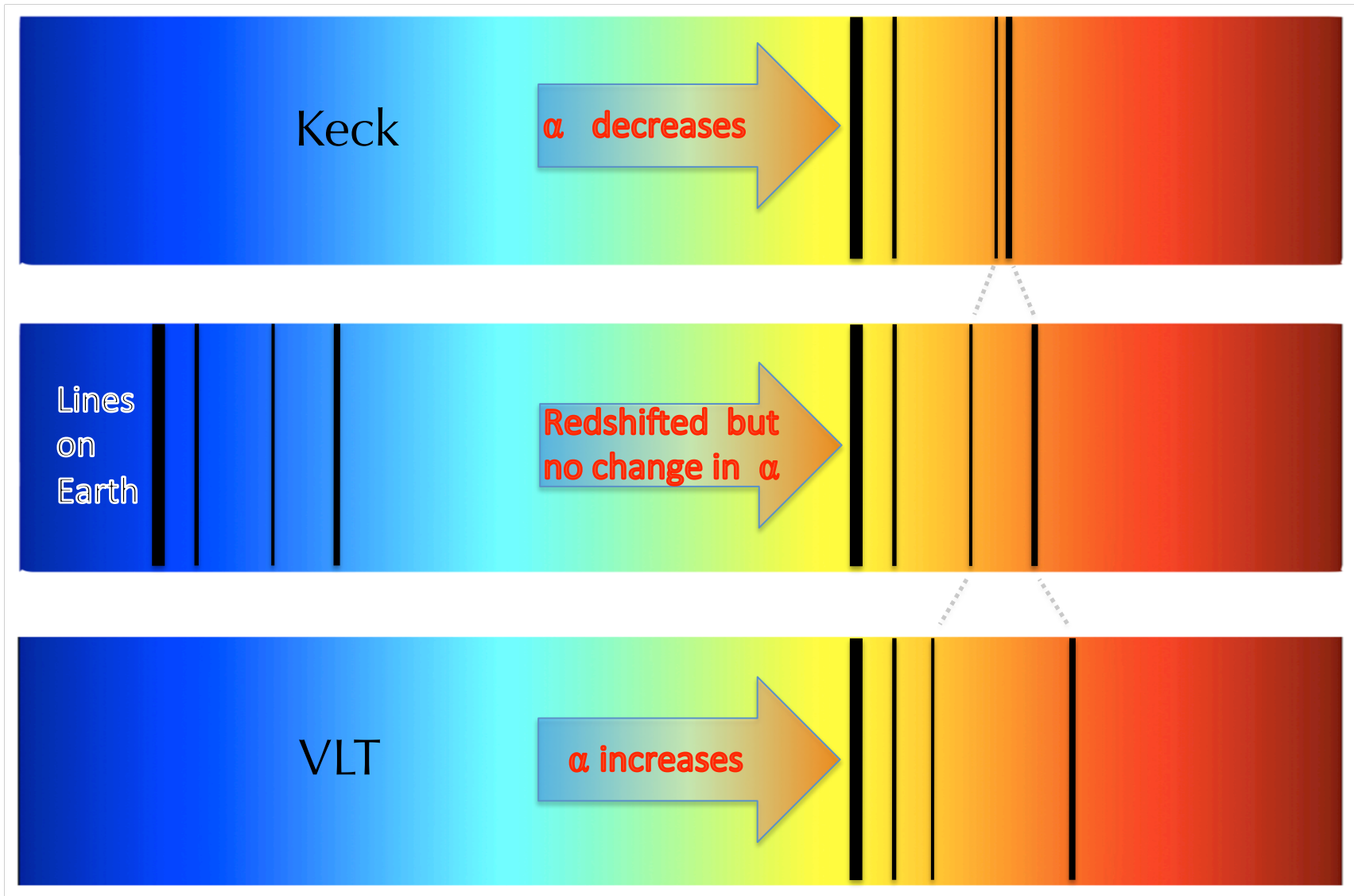
Redshift (z)

300 measurements. No other comparable sample YET...

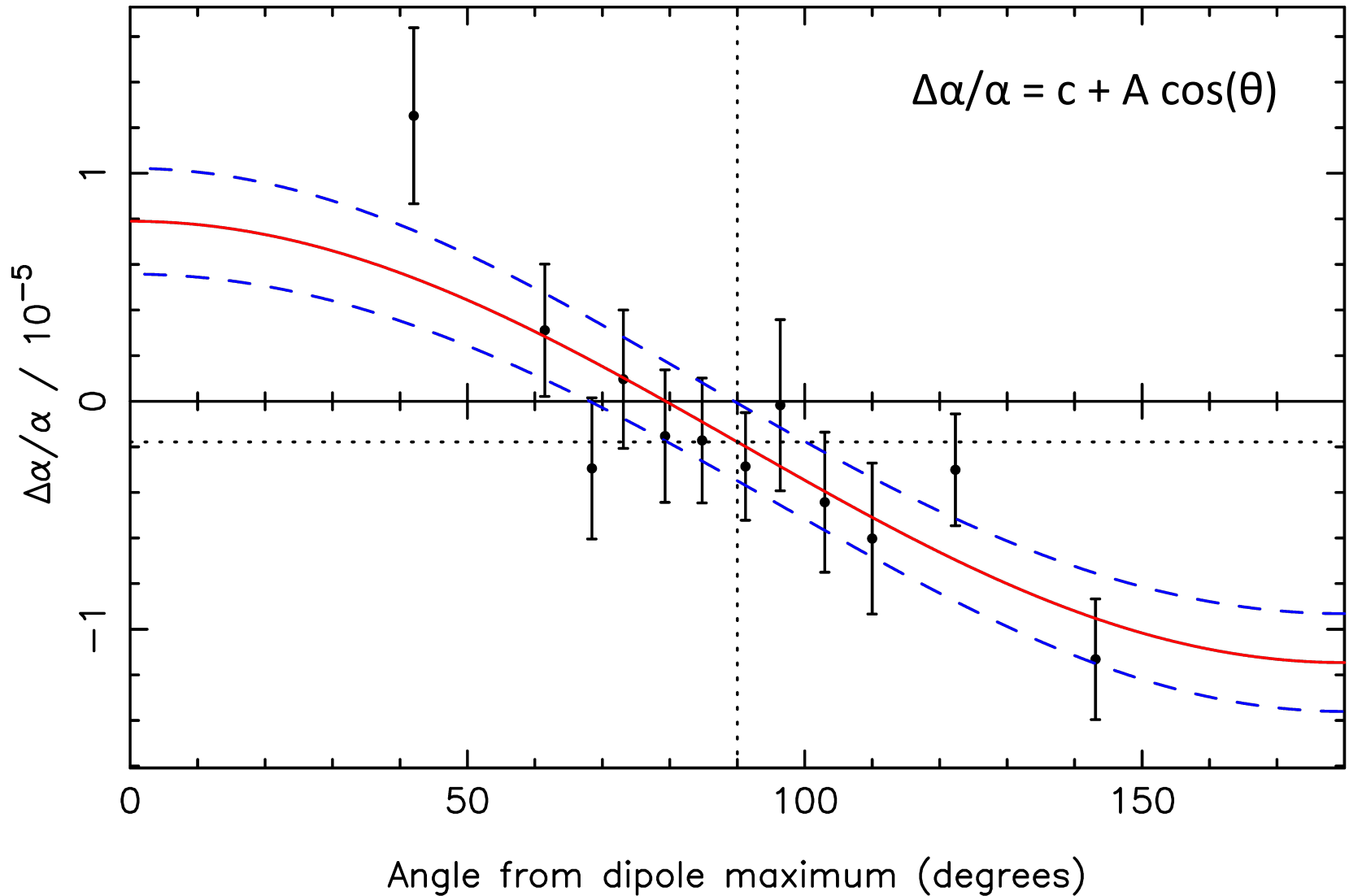


$$\omega_z = \omega_0 + Q (\alpha_z^2 - \alpha_0^2) / \alpha_0^2$$

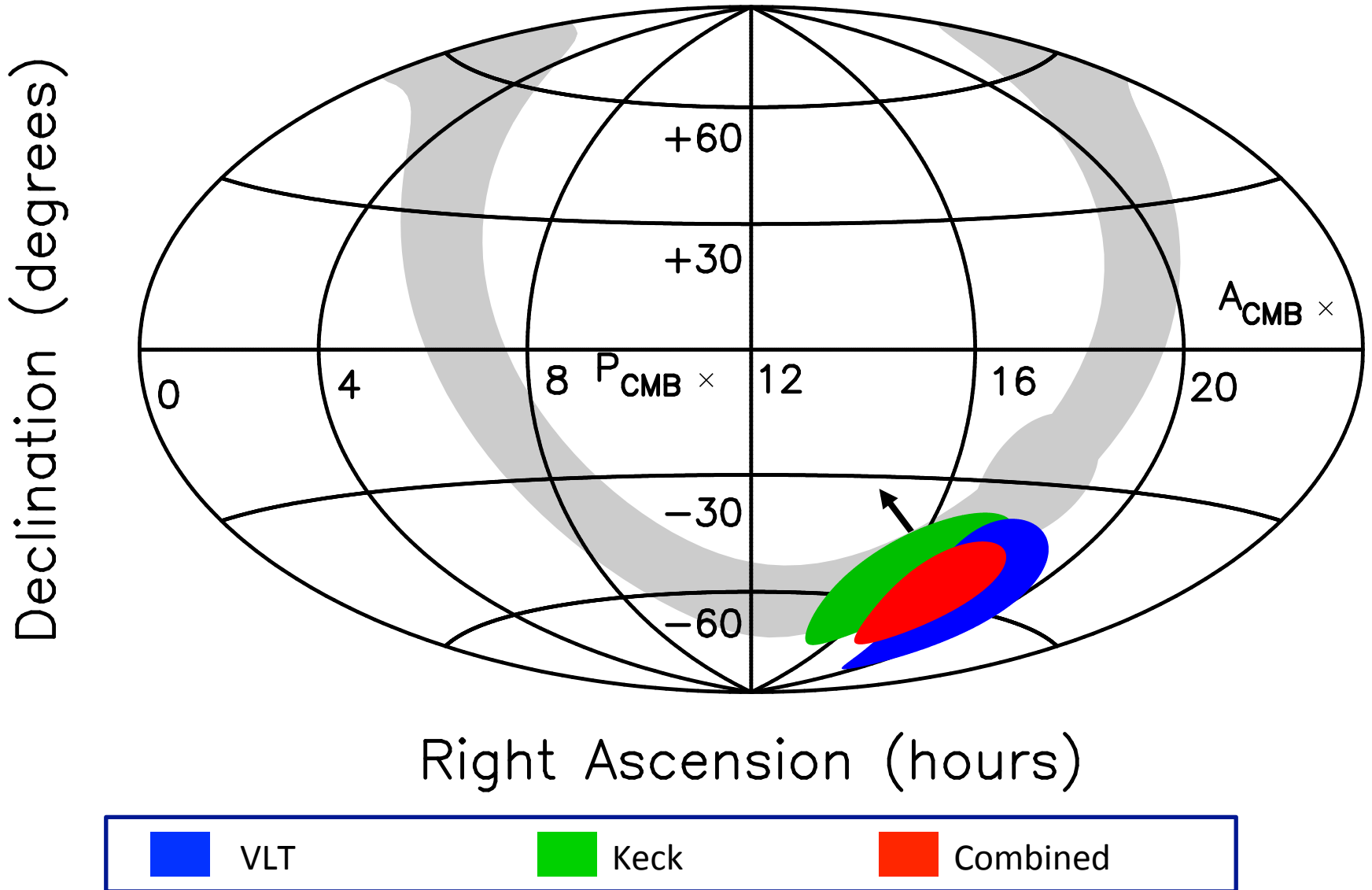
Different *patterns* in different directions



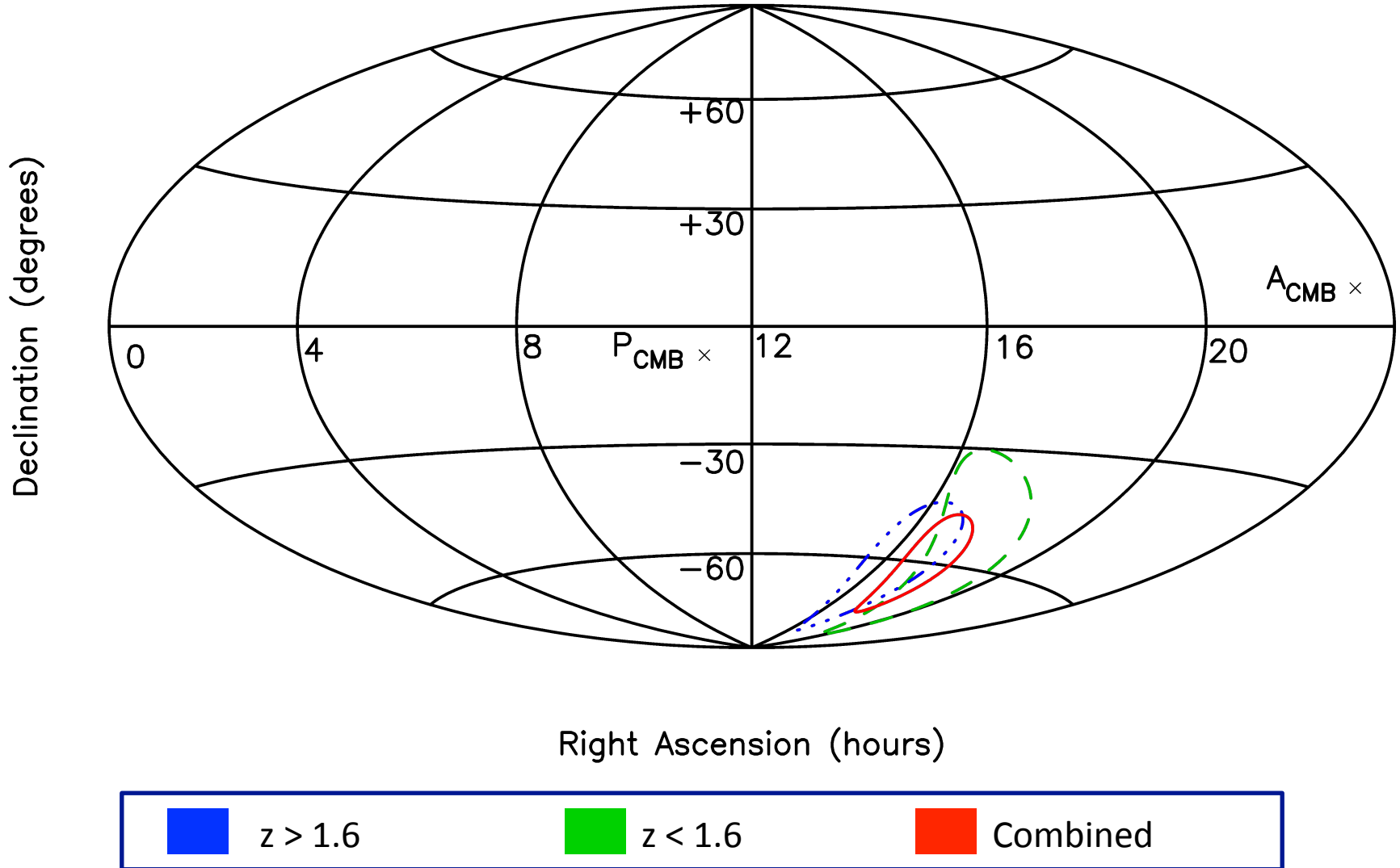
4.2 σ evidence for a $\Delta\alpha/\alpha$ dipole from VLT + Keck



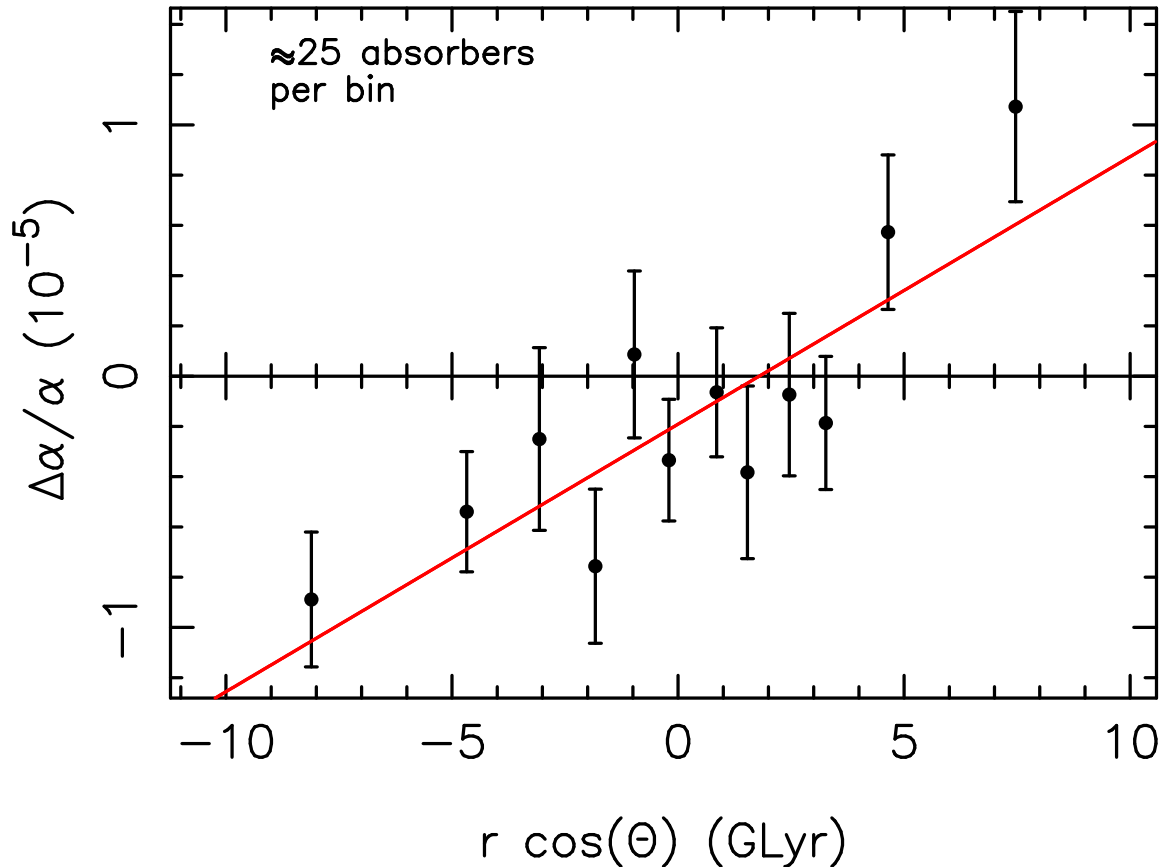
Keck & VLT dipoles independently agree, $p=6\%$



Low and high redshift cuts are consistent in direction.
Effect is larger at high redshift.



Distance dependence

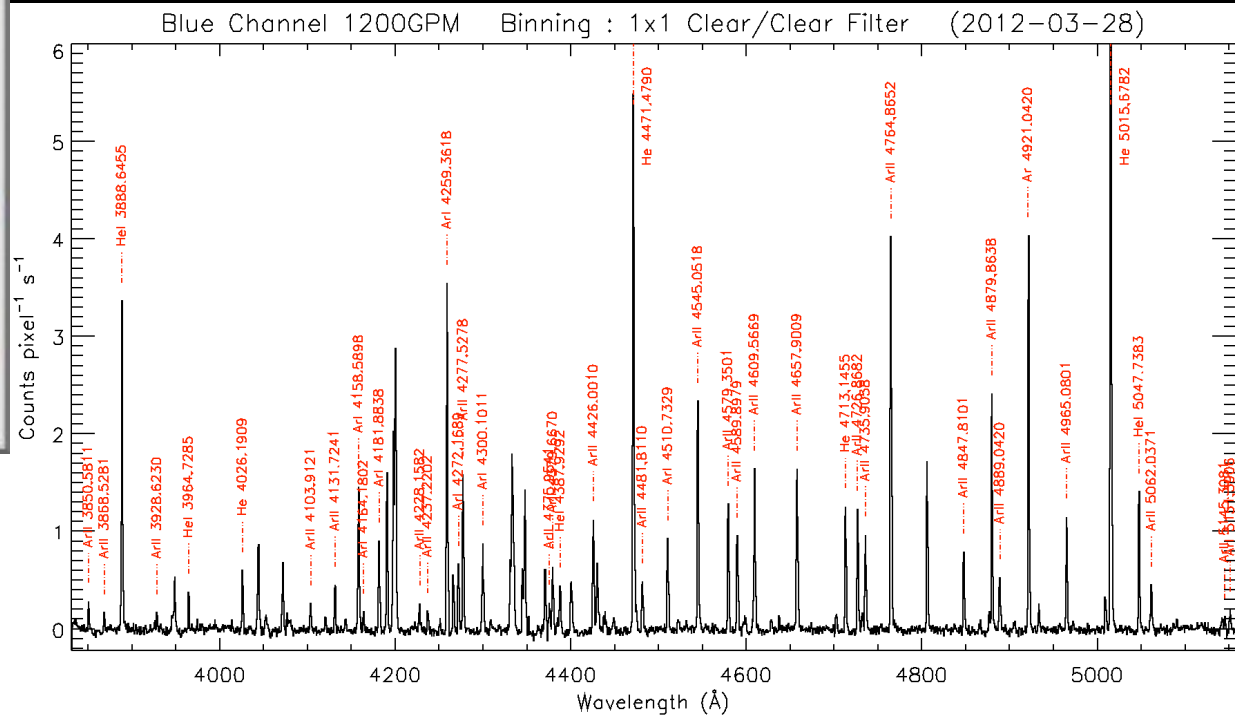


$\Delta\alpha/\alpha$ vs $B r \cos\theta$ for the model $\Delta\alpha/\alpha = B r \cos\theta + m$ showing the gradient in α along the best-fit dipole. The best-fit direction is at right ascension 17.4 ± 0.6 hours, declination -62 ± 6 degrees, for which $B = (1.1 \pm 0.2) \times 10^{-6} \text{ GLyr}^{-1}$ and $m = (-1.9 \pm 0.8) \times 10^{-6}$. This dipole+monopole model is statistically preferred over a monopole-only model also at the 4.2σ level. A cosmology with parameters $(H_0, \Omega_M, \Omega_\Lambda) = (70.5, 0.2736, 0.726)$.

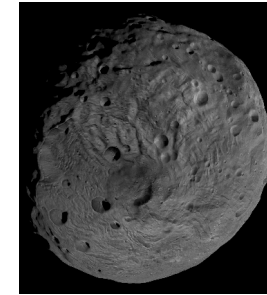
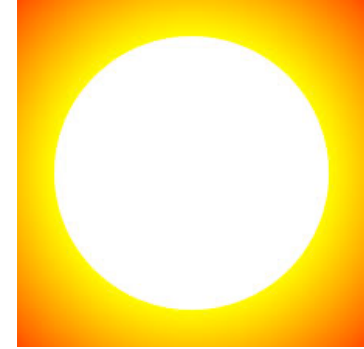
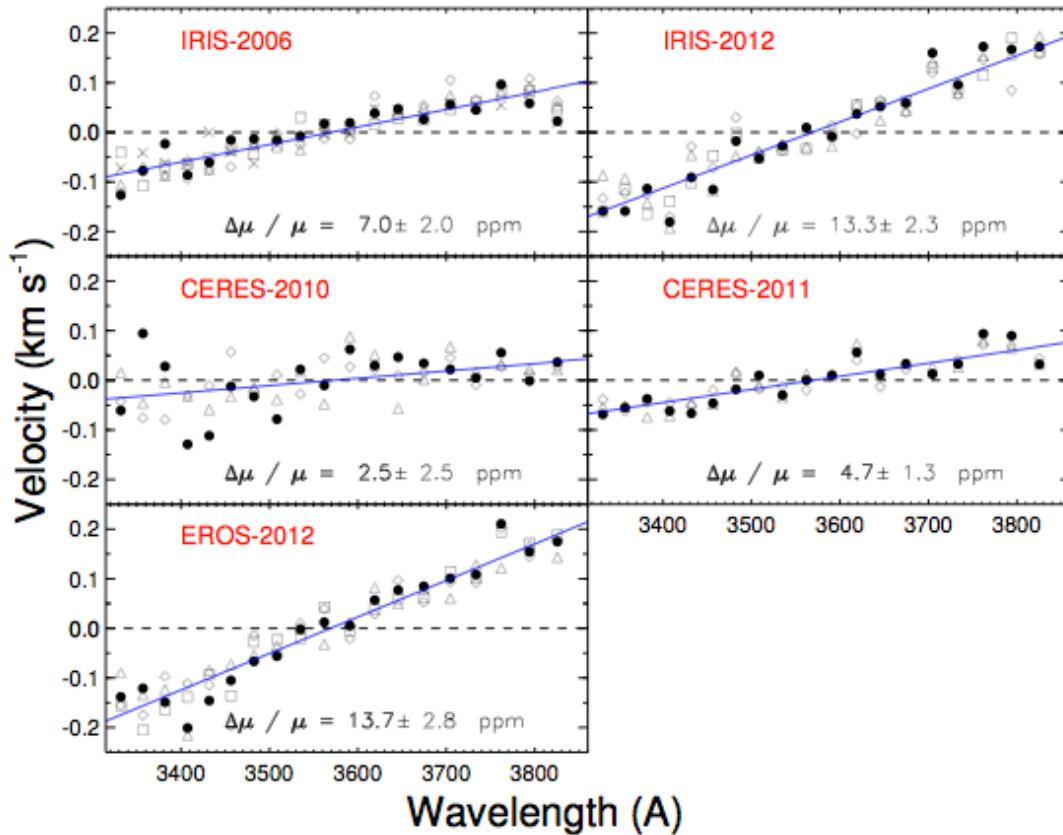


Wavelength calibration

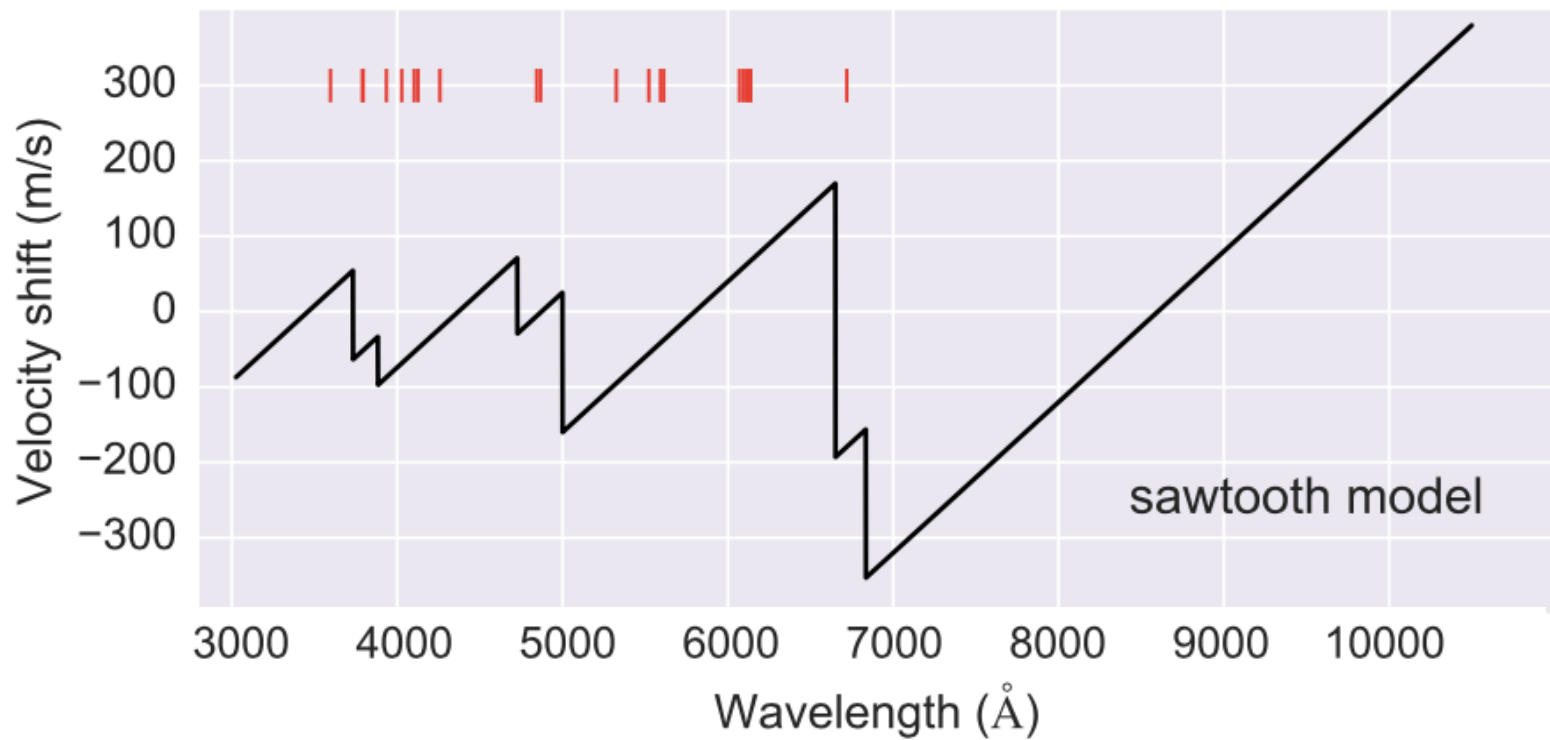
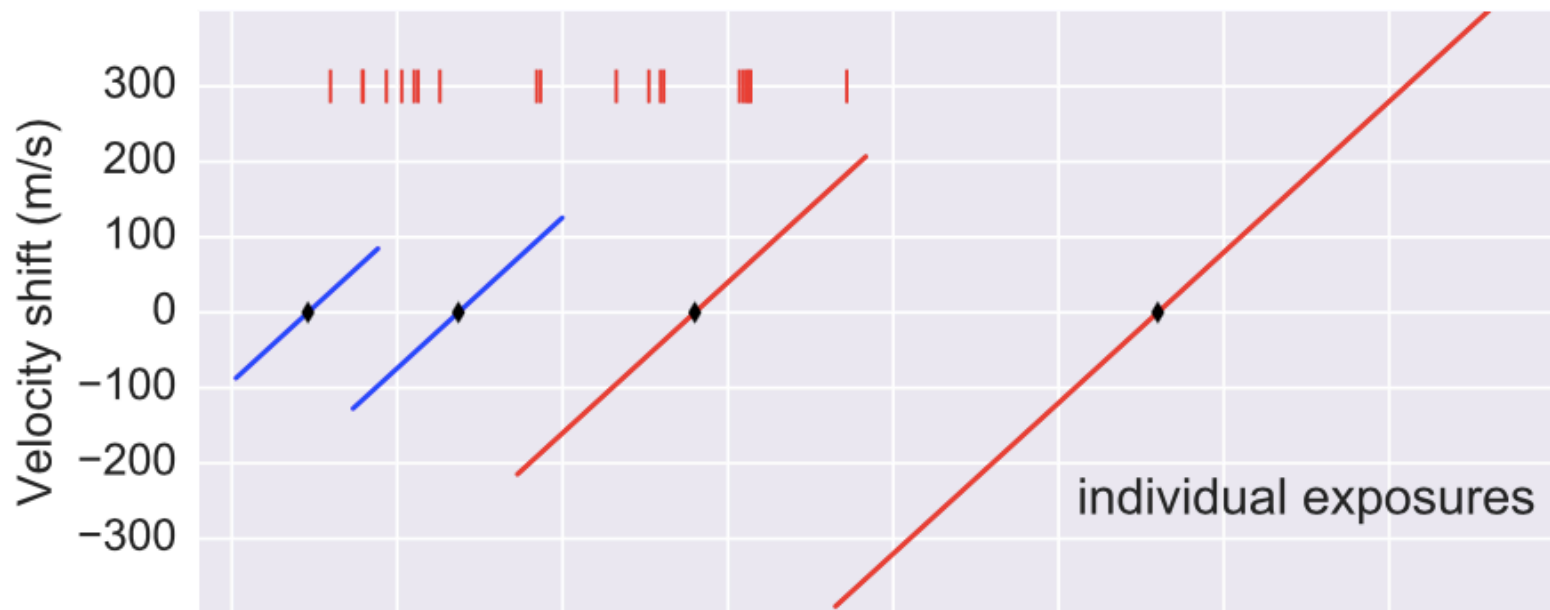
Thorium-Argon lamps at telescope.



Evidence for large-scale wavelength distortions



Note the zero point is at the central wavelength



Distortion does not explain the VLT results

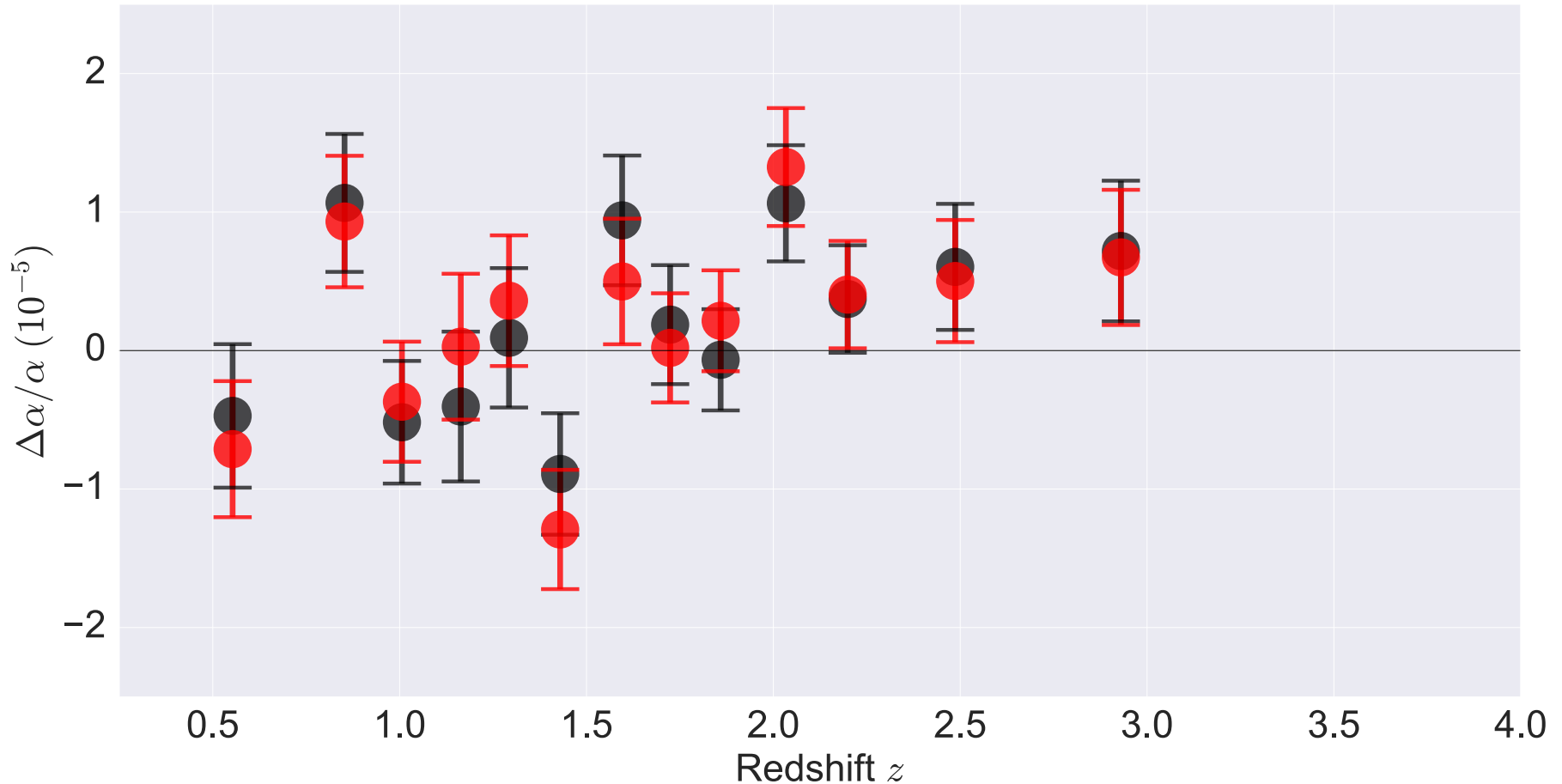
1. [arXiv:1701.03176](#) [pdf, other]

Modeling long-range wavelength distortions in quasar absorption echelle spectra

Vincent Dumont, John K. Webb

Comments: 8 pages, 7 figures, 3 tables

Subjects: **Cosmology and Nongalactic Astrophysics (astro-ph.CO)**



BLACK: Original results – no distortion correction

RED: Distortion corrected results

Removing the human element – applying AI to varying constants

New method, combining three procedures into one AI process:

- Genetic algorithm
- Local non-linear least-squares
- Bayesian model averaging

2. [arXiv:1606.07393](#) [pdf, other]

Artificial intelligence applied to the automatic analysis of absorption spectra. Objective measurement of the fine structure constant

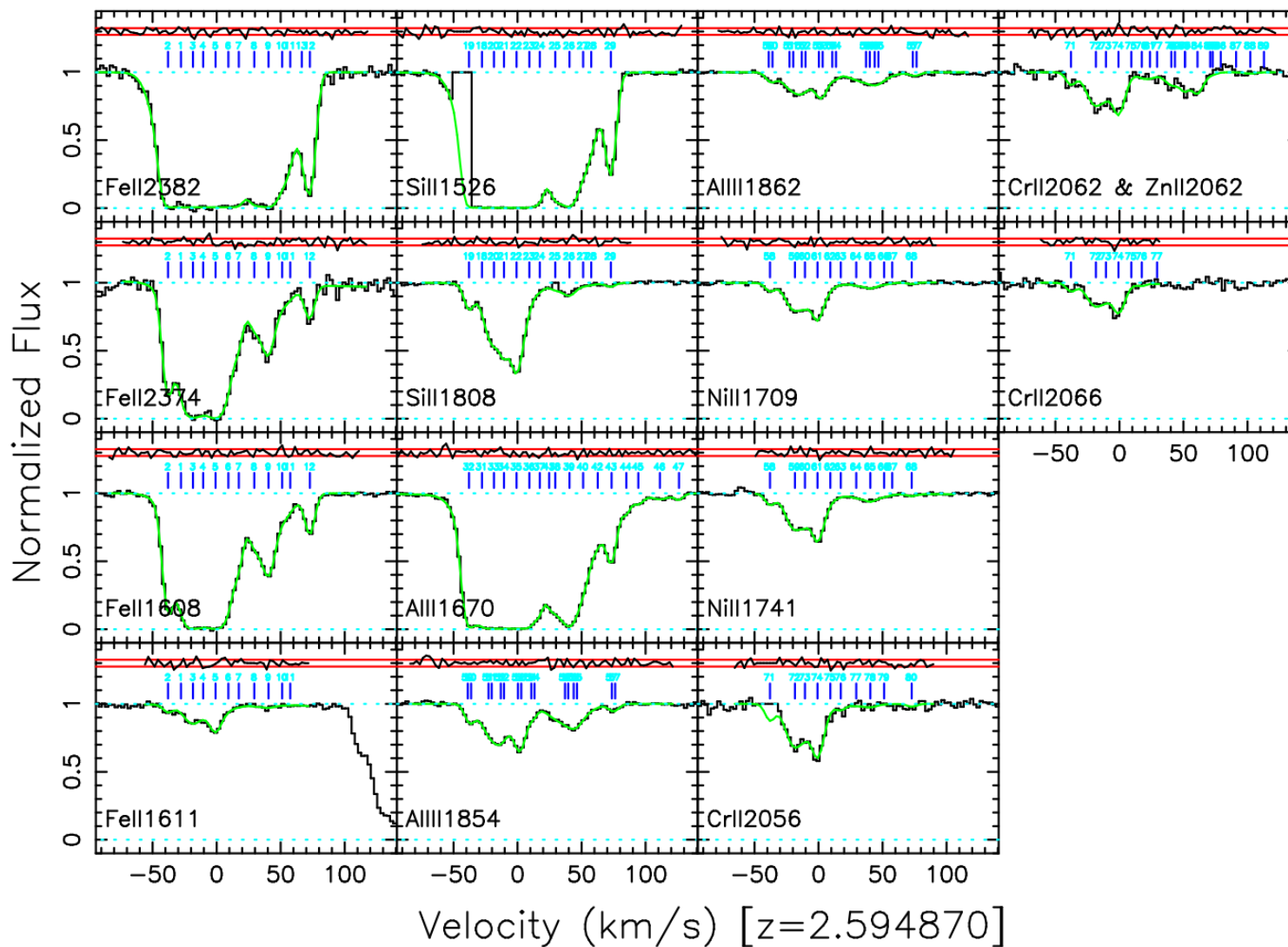
[Matthew B. Bainbridge](#), [John K. Webb](#)

Comments: 34 pages, 10 figures, 16 tables. Submitted to MNRAS

Subjects: Instrumentation and Methods for Astrophysics (astro-ph.IM)

The challenge: complicated data – need models with many free (and tied) parameters

J040718–441013 $z=2.595$



INITIALISATION

- * Set all atomic data;
- * Identify atomic species to be fitted;
- * Define instrumental spectral resolution;
- * Define M spectral ranges to be fitted;
- * Set up all free and tied fitting parameters;
- * Define genetic search first-guess parameter ranges, step sizes, stopping criteria;
- * Initialise the population (i.e. create N "empty" spectral segments).

REPRODUCTION

- * Set up the current "parents" - populate the MxN spectral segments with first-guess models (at iteration zero this is a single absorption line. The model complexity increases with subsequent generations).

MUTATION

- * Increase model complexity - add an additional absorption component.

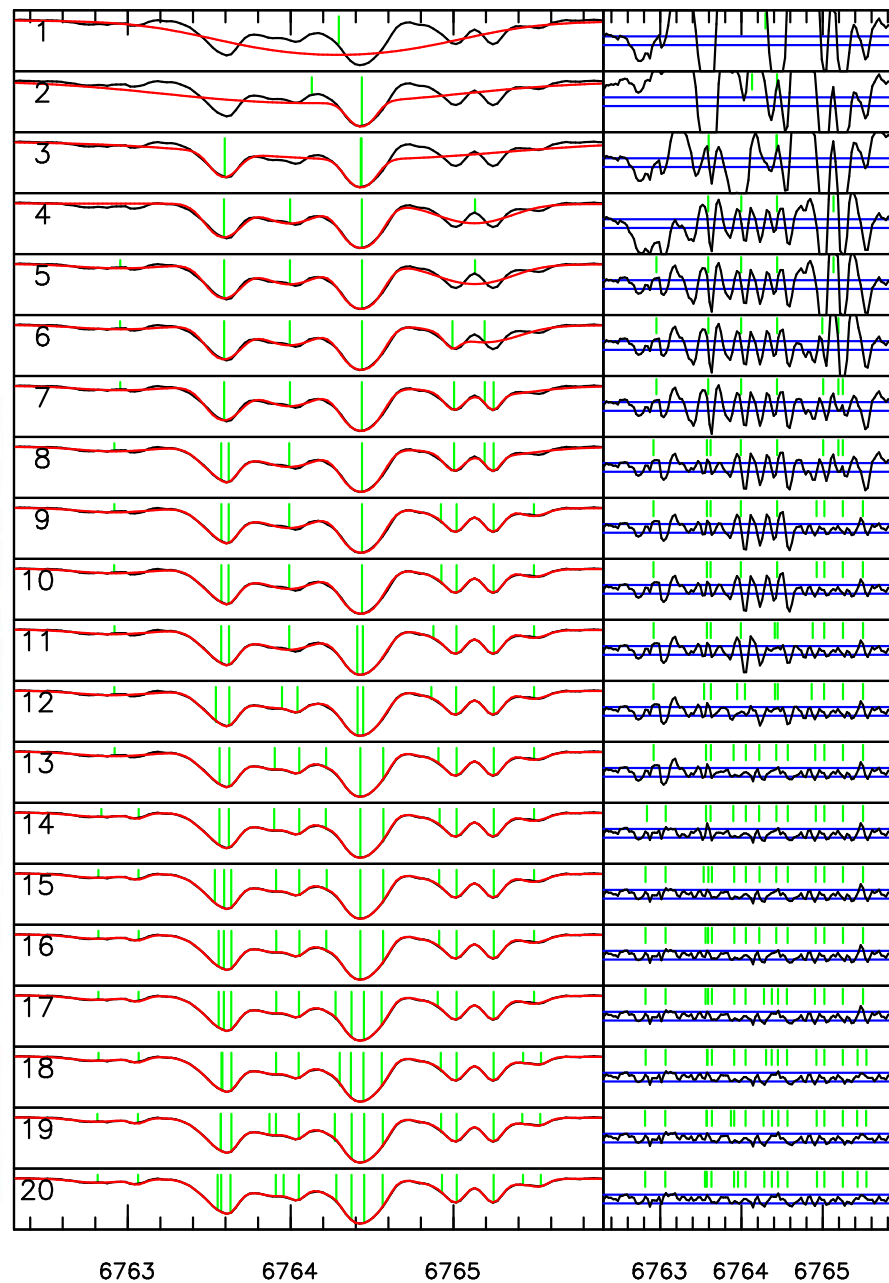
Local non-linear least-squares optimisation of all MxN models (VPFIT)

SELECTION

- * From the MxN, pick the "fittest", lowest chi-squared, model.

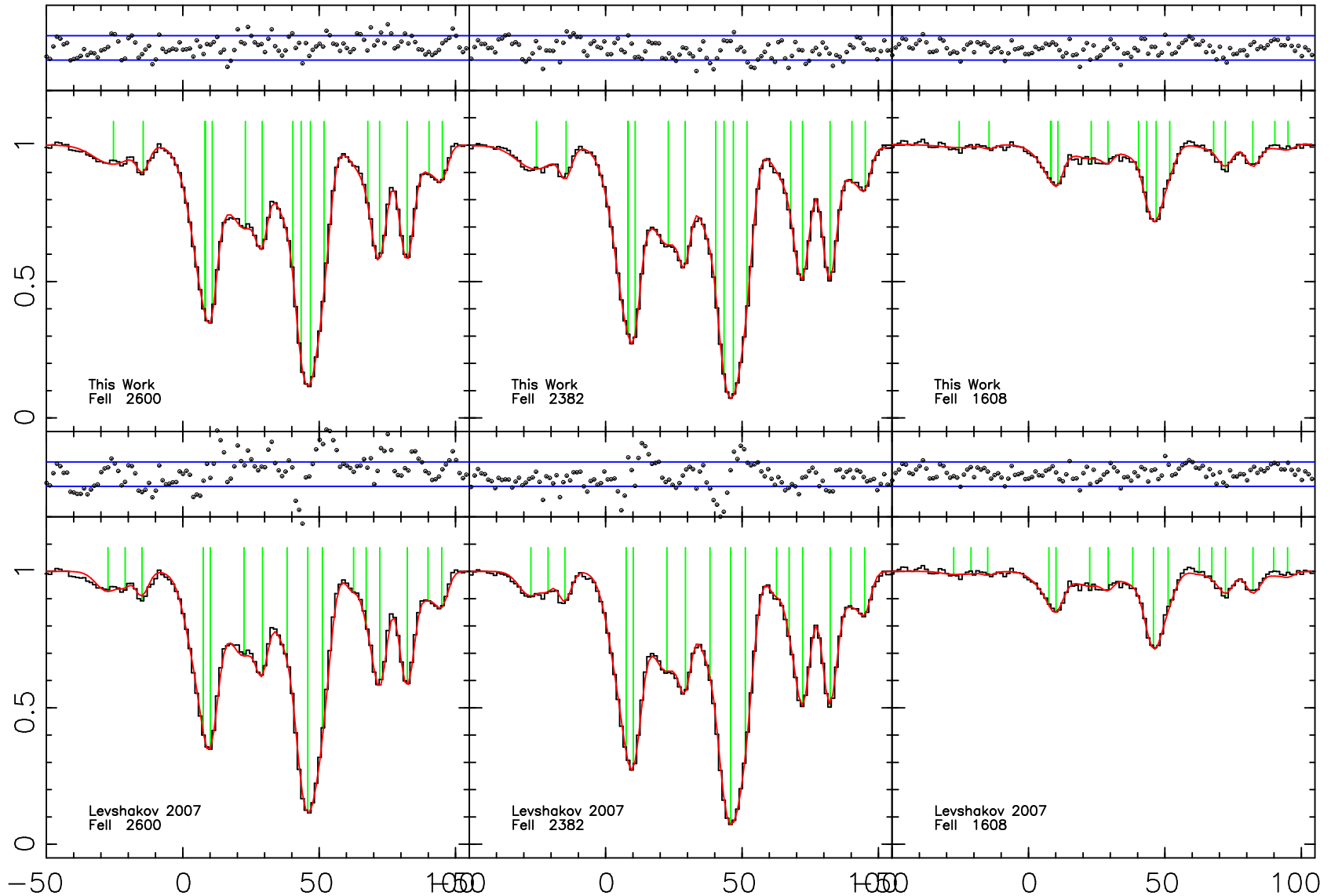
EVOLUTION

- * Check selected model against stopping criteria;
- * If stopping criteria not met, current model becomes the new "parent".

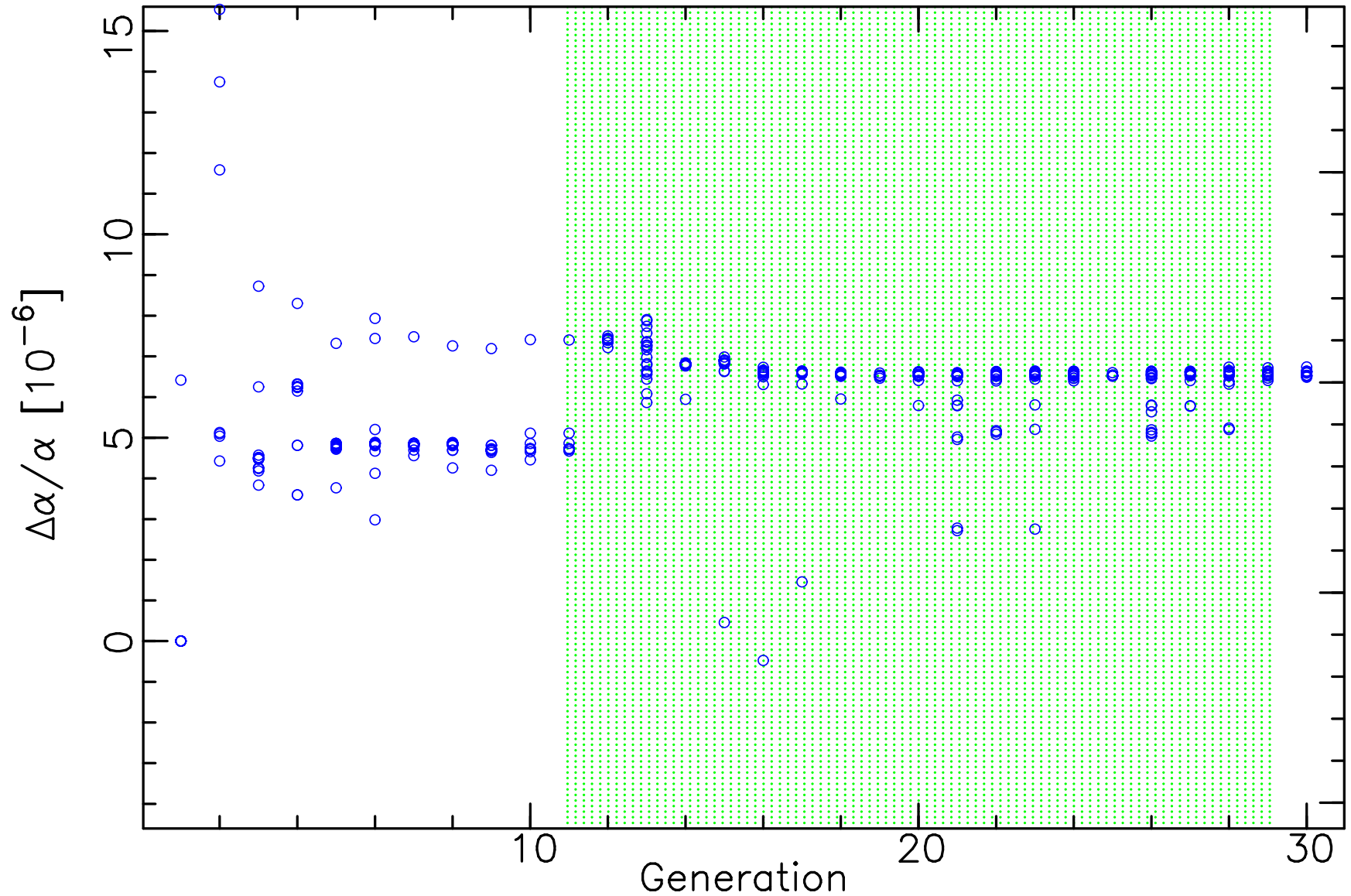


Wavelength (Å)

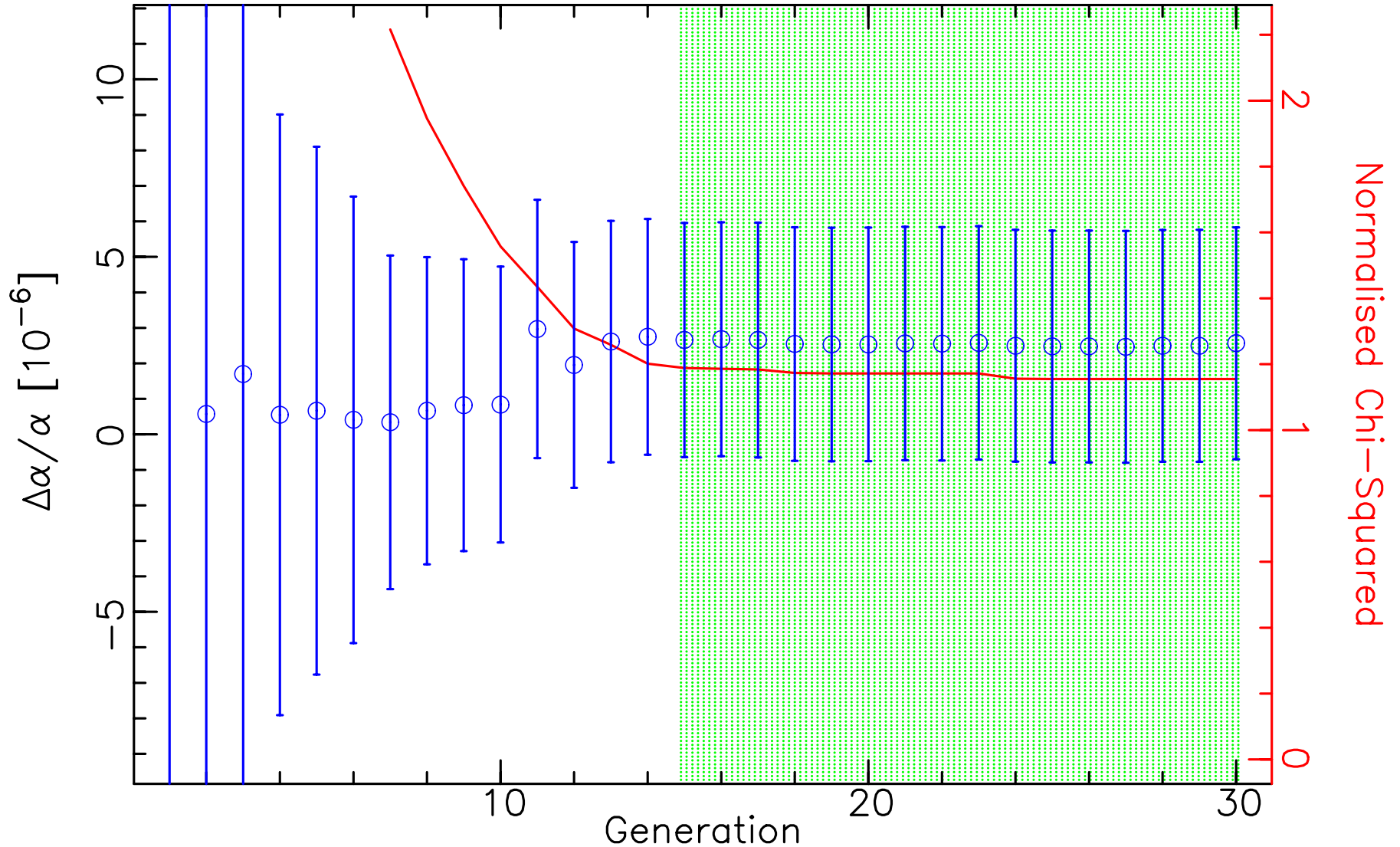
A genetic algorithm doesn't necessarily emulate what a human does – no unique model!



Every generation has a distribution of candidate $\Delta\alpha/\alpha$ solutions



$\Delta\alpha/\alpha$ solution is stable to first guesses and probably stable to small changes in the model



The first 1000 new measurements of the fine structure constant at high redshift using AI

Approximate many-multiplet sample sizes:

Already published: 300

Currently: Up to about 600 many multiplets + lots of doublets

Possible using existing archival data: ~1500



“Raijin” (named after the Shinto God of thunder, lightning and storms)
National Computational Infrastructure, ANU, Canberra, Australia



**January-June 2017:
230,000 hours on “Raijin”, the world’s 24th most powerful computer**

- 57,864 cores (Intel Xeon Sandy Bridge technology, 2.6 GHz) in 3602 compute nodes
- 56 NVIDIA Tesla K80 GPUs
- 162 TBytes of main memory
- Mellanox FDR 56 Gb/sec Infiniband full fat tree interconnect
- 12.5 PBytes of high-performance operational storage capacity
- This provides a peak performance of approximately 1.37 Pflops

420 newly available spectra from Keck and VLT archive

SUBMITTED TO THE ASTRONOMICAL JOURNAL
Preprint typeset using L^AT_EX style emulateapj v. 5/2/11

THE FIRST DATA RELEASE OF THE KODIAQ SURVEY

J.M. O'MEARA¹, N. LEHNER², J.C. HOWK², J.X. PROCHASKA³, A.J. FOX⁴, M. A. SWAIN⁵, C. R. GELINO⁶, G. B. BERRIMAN⁶, & H. TRAN⁷

Submitted to the Astronomical Journal

ABSTRACT

We present and make publicly available the first data release (DR1) of the Keck Observatory Database of Ionized Absorption toward Quasars (KODIAQ) survey. The KODIAQ survey is aimed at studying galactic and circumgalactic gas in absorption at high-redshift, with a focus on highly-ionized gas traced by O VI, using the HIRES spectrograph on the Keck-I telescope. KODIAQ DR1 consists of a fully-reduced sample of 170 quasars at $0.29 < z_{\text{em}} < 5.29$ observed with HIRES at high resolution ($36,000 \leq R \leq 103,000$) between 2004 and 2012. DR1 contains 247 spectra available in continuum normalized form, representing a sum total exposure time of ~ 1.6 megaseconds. These coadded spectra arise from a total of 567 individual exposures of quasars taken from the Keck Observatory Archive (KOA) in raw form and uniformly processed using a HIRES data reduction package made available through the XIDL distribution. DR1 is publicly available to the community, housed as a higher level science product at the KOA. We will provide future data releases that make further QSOs, including those with pre-2004 observations taken with the previous-generation HIRES detectors.

Subject headings: absorption lines – intergalactic medium – Lyman limit systems – damped Lyman alpha systems

The ESO UVES Advanced Data Products Quasar Sample - I. Dataset and New N_{HI} Measurements of Damped Absorbers

Tayyaba Zafar¹, Attila Popping², and Céline Péroux¹

¹ Aix Marseille Université, CNRS, LAM (Laboratoire d'Astrophysique de Marseille) UMR 7326, 13388, Marseille, France.

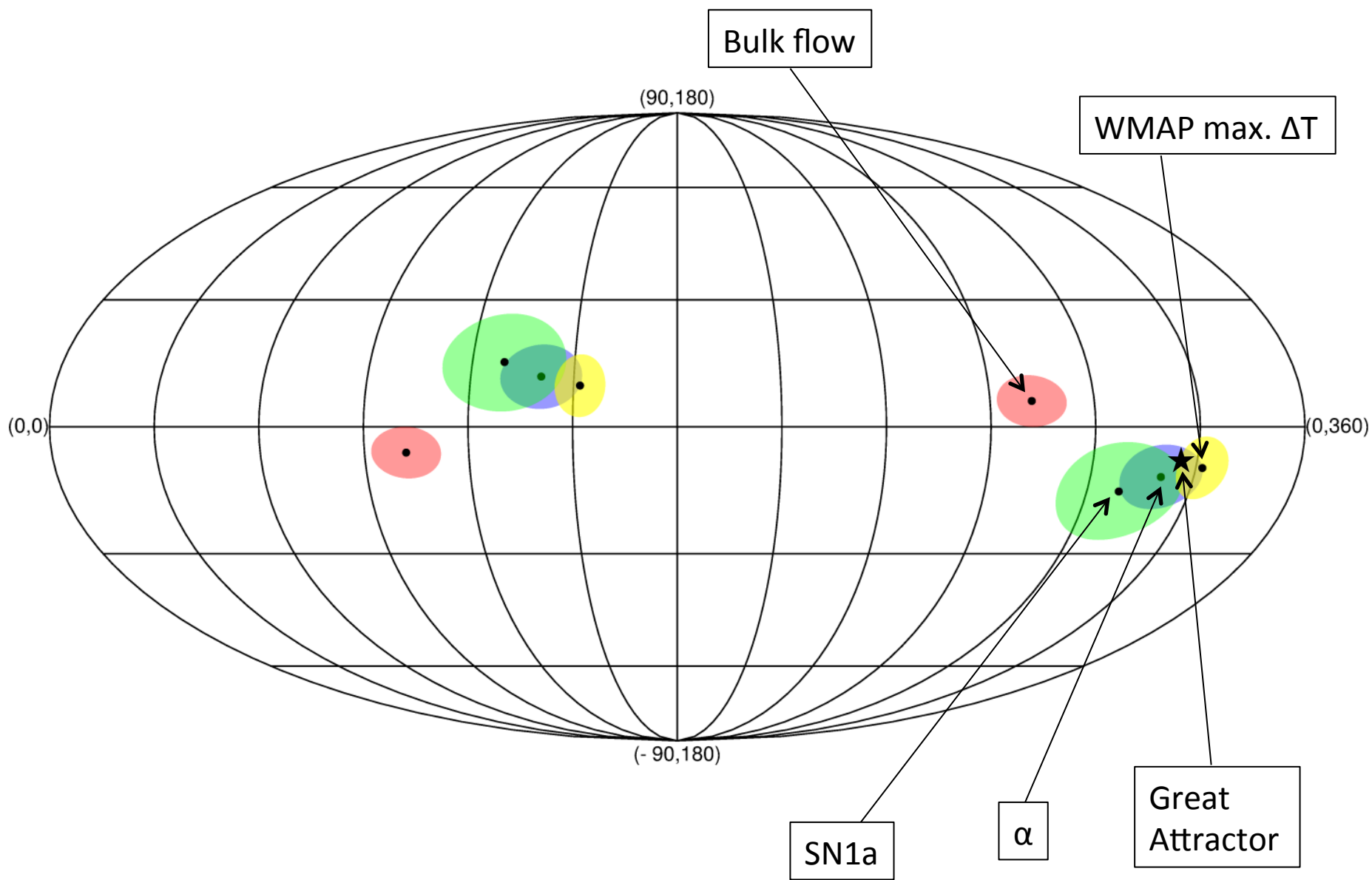
² International Centre for Radio Astronomy Research (ICRAR), The University of Western Australia, 35 Stirling Hwy, Crawley, WA 6009, Australia.

Received / Accepted

ABSTRACT

We present here a dataset of quasars observed with the Ultraviolet Visual Echelle Spectrograph (UVES) on the Very Large Telescope and available in the European Southern Observatory UVES Advanced Data Products archive. The sample is made up of a total of 250 high resolution quasar spectra with emission redshifts ranging from $0.191 \leq z_{em} \leq 6.311$. The total UVES exposure time of this dataset is 1560 hours. Thanks to the high resolution of UVES spectra, it is possible to unambiguously measure the column density of absorbers with damping wings, down to $N_{HI} \gtrsim 10^{19} \text{ cm}^{-2}$, which constitutes the sub-damped Ly α absorber (sub-DLA) threshold. Within the wavelength coverage of our UVES data, we find 150 damped Ly α systems (DLAs)/sub-DLAs in the range $1.5 < z_{obs} < 4.7$. Of these 150, 93 are DLAs and 57 are sub-DLAs. An extensive search in the literature indicates that 6 of these DLAs and 13 of these sub-DLAs have their N_{HI} measured for the first time. Among them, 10 are new identifications as DLAs/sub-DLAs. For each of these systems, we obtain an accurate measurement of the HI column density and the absorber's redshift in the range $1.7 < z_{obs} < 4.2$ by implementing a Voigt profile-fitting algorithm. These absorbers are further confirmed thanks to the detection of associated metal lines and/or lines from members of the Lyman series. In our data, a few quasars' lines-of-sight are rich. An interesting example is towards QSO J0133+0400 ($z_{em} = 4.154$) with six DLAs and sub-DLAs reported.

Key words. Galaxies: abundances – Galaxies: high-redshift – Quasars: absorption lines – Quasars: general.



Conclusions

1. We have hints of spatial variation from the largest available sample of high redshift measurements of alpha. More measurements are on the way. Of course, independent methods are highly desirable.
2. Long-range wavelength distortions do not explain the putative dipole.
3. A fully-automated AI method has been developed which does better than a human, permitting a far larger sample of measurements and removing any possible bias.
4. Supercomputer calculations are currently being done to produce the first 1000 cosmological measurements of alpha.
5. VPFIT is being improved in terms of precision of Voigt function and Voigt derivative precisions. This should improve robustness and accuracy of error estimates.